Published June 20, 2011

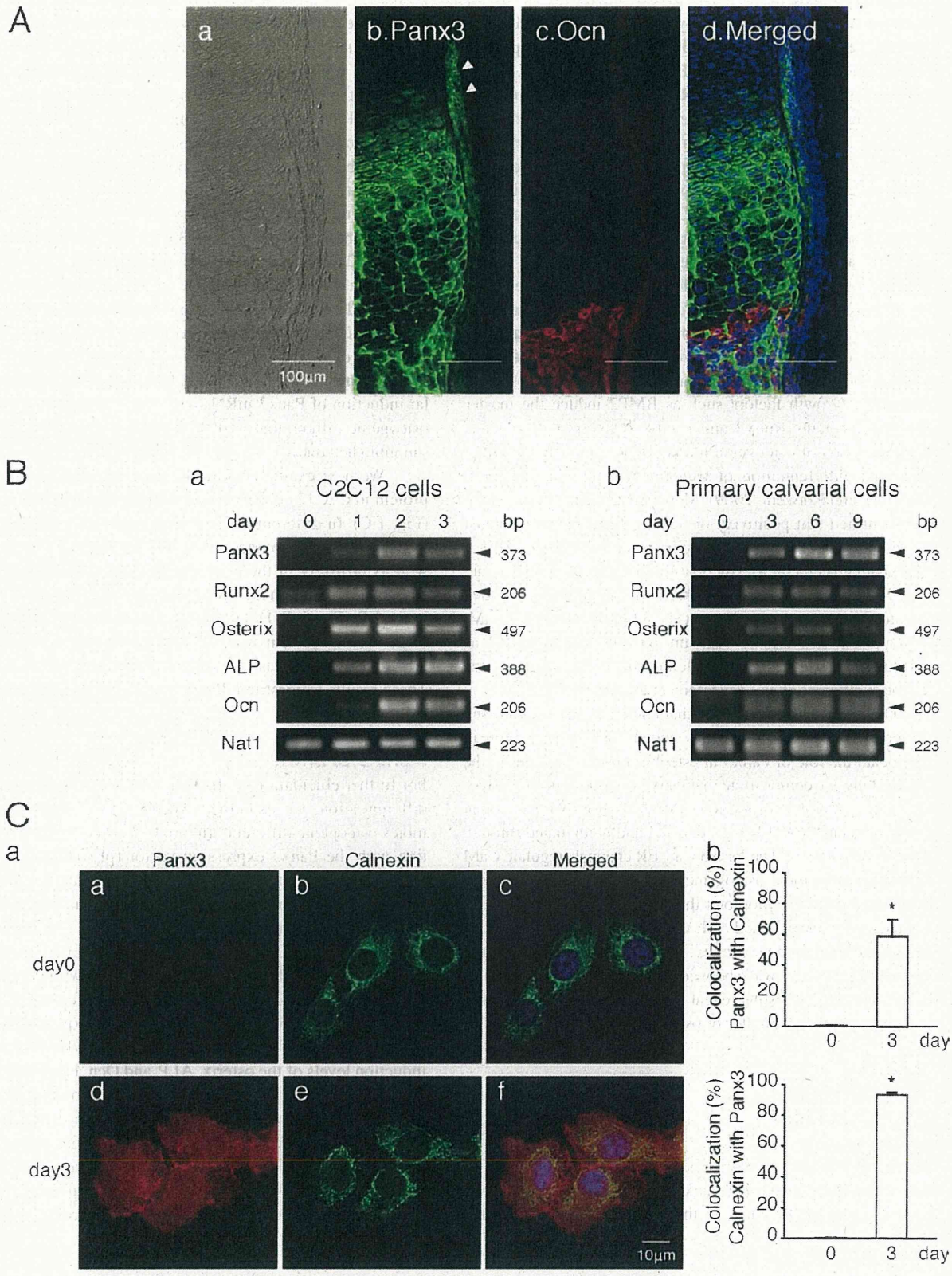

Figure 1. **Expression of Panx3 in growth plates, C2C12 cells, and primary calvarial cells.** (A) Immunostaining of newborn mouse growth plates. Image under light microscopy (a), Panx3 (b), Ocn (c), Hoechst nuclear staining (blue), and merged image (d). Arrowheads, perichondrium/periosteum. (B) Semi-quantitative RT-PCR. C2C12 cells (a) and primary calvarial cells (b) were cultured with BMP2 and ascorbate, respectively, at day 0. Panx3 was induced

Downloaded from jcb.rupress.org on May 6, 2012

organelle, when cells are activated by extracellular stimuli. Inositol trisphosphate 3 (IP3) receptors (IP3Rs) are ubiquitously expressed and act as ER Ca^{2+} channels upon IP3 binding (Mikoshiba, 2007). IP3 synthesis for activation of IP3R ER channels can be induced by many stimuli. For example, external ATP can bind purinergic receptors (P2Rs) in the plasma membrane, and this triggers activation of phospholipase C (PLC) and subsequent IP3 generation. Ryanodine receptors (RyRs) are also known to function as ER Ca^{2+} channels in some tissues (Fill and Copello, 2002). More recently, Panx1 was unexpectedly found to function as an ER Ca^{2+} channel in prostate cancer cells (Vanden Abeele et al., 2006).

The Ca^{2+} binding protein calmodulin (CaM) is one of the major Ca^{2+} signaling mediators (Berridge et al., 2000b), and the CaM pathway regulates osteoblast differentiation (Zayzafoon, 2006). Osteoblasts differentiate from mesenchymal stem cells and form bone through endochondral and intramembranous ossification. Growth factors such as BMP2 induce the master osteogenic proteins Runx2 and osterix (Osx/Sp7). This leads to the activation of osteogenic marker genes, and subsequently, to terminal differentiation of osteoblasts (Fujita et al., 2004; Mukherjee and Rotwein, 2009). Many signaling molecules have been identified that positively or negatively regulate osteoblast differentiation. For example, phosphoinositide 3-kinase (PI3K)/Akt signaling is crucial for osteoblast differentiation (Fujita et al., 2004; Mukherjee and Rotwein, 2009), whereas p53 is a negative regulator for osteogenesis (Wang et al., 2006). In the case of CaM, binding to Ca^{2+} activates downstream signaling molecules such as CaM kinase II (CaMKII) and calcineurin (CN), and promotes osteoblast differentiation (Zayzafoon et al., 2005).

Our previous study showed that Panx3 mRNA is expressed in osteoprogenitors and osteoblasts, and prompted us to explore in more detail the role of Panx3 in osteoblast differentiation. In the present study, we demonstrate that Panx3 is induced during osteoblast differentiation and promotes differentiation. We found that Panx3 functions as an ER Ca^{2+} channel and is regulated through a PI3K–Akt pathway. The Panx3 Ca^{2+} ER channels regulate CaM pathways and promote osteogenic differentiation. Panx3, acting as a hemichannel, also promotes the release of ATP into the extracellular space. The released ATP may bind to P2Rs followed by activation of PI3K–Akt signaling. Furthermore, Panx3 gap junctions propagate a Ca^{2+} wave between cells and enhance osteoblast differentiation. Our results reveal that Panx3 plays a multifunctional role as a new regulator of osteoblast differentiation.

Results

Panx3 expression and localization in growth plates and differentiating osteoblasts

We previously reported that Panx3 mRNA is expressed in prehypertrophic chondrocytes, in the perichondrium/periosteum, and in osteoblasts in the growth plate (Iwamoto et al., 2010). Immunohistochemistry showed that the Panx3 protein was expressed in prehypertrophic and hypertrophic chondrocytes, as well as in the perichondrium/periosteum, which are progenitors for osteoblasts (arrowheads in Fig. 1 A, b). Immunostaining of osteocalcin (Ocn), an osteoblast marker, showed a distinct boundary between cartilage and bone. Panx3 was also expressed in osteoblasts (Fig. 1 A, c and d).

To study the role of Panx3 in osteoblast differentiation, we analyzed the expression of Panx3 mRNA in the osteoprogenitor cell line C2C12, and in primary calvarial cells from newborn mice (Fig. 1 B). Panx3 mRNA was not detectable in undifferentiated cells. However, when the cells differentiated into osteoblasts, Panx3 expression was found concomitantly with the induction of osteoblast marker genes such as Runx2, osterix, alkaline phosphatase (ALP), and Ocn (Fig. 1 B, a and b). Similar induction of Panx3 mRNA expression was observed during osteogenic differentiation of MC3T3-E1 and C3H10T1/2 cells (unpublished data).

We next examined subcellular localization of the Panx3 protein in C2C12 cells using fluorescence confocal microscopy (Fig. 1 C). In differentiating C2C12 cells, Panx3 was localized to the plasma membrane and within cell–cell contact areas, as well as diffusely in the cytosol. Calnexin, an ER marker, was colocalized with Panx3, which suggests that Panx3 is localized in the ER (Fig. 1 C, f). Quantitative analysis revealed that 60% of the Panx3 protein was colocalized with calnexin, whereas 90% of calnexin was colocalized with Panx3 (Fig. 1 C, b). These results suggest that Panx3 may function at multiple subcellular regions.

Panx3 promotes osteoblast differentiation

For further elucidation of the Panx3 function during osteoblast differentiation, we examined whether Panx3 expression promotes osteogenic differentiation of C2C12 cells. After transfection with the Panx3 expression vector (pEF1/Panx3; Fig. S1, A and B), C2C12 cells were induced to differentiate, and mRNA expression of osteoblast marker genes was analyzed over time using real-time quantitative PCR (Fig. 2 A). The expression of osterix, ALP, and Ocn was increased in Panx3-overexpressing cells compared with control cells transfected with vector pEF1, whereas the Runx2 expression level was unaffected in both cell types (Fig. 2 A). When endogenous Panx3 expression was inhibited by shPanx3 RNA transfection (Fig. S1, A and B), the induction levels of the osterix, ALP, and Ocn, but not of Runx2, were reduced (Fig. 2 B). Panx3 overexpression also promoted ALP activity and mineralization, whereas suppression of endogenous Panx3 by shPanx3 inhibited these processes (Fig. 2, C and D). We observed similar results in primary calvarial cells (Fig. S2, A, B, and C). Collectively, these findings indicated that Panx3 promotes osteoblast differentiation processes.

during osteoblast differentiation in both cell types. Runx2, osterix, ALP, and Ocn are osteoblast differentiation marker genes. Nat1 was used as a control. (C, a) Cellular localization of endogenous Panx3 in undifferentiated (a–c) and differentiated C2C12 cells (d–f) after 4 d of culture with BMP2. Panx3 (red) was localized in the plasma membrane, cell–cell junctions, and ER membranes in differentiated cells. Calnexin was used as an ER marker. (b) Measurements show a percentage of colocalization between Panx3 with calnexin (top), and calnexin with Panx3 (bottom). *, $P < 0.05$. Error bars represent the mean ± SD; $n = 12$.

Downloaded from jcb.rupress.org on May 6, 2012

Published June 20, 2011

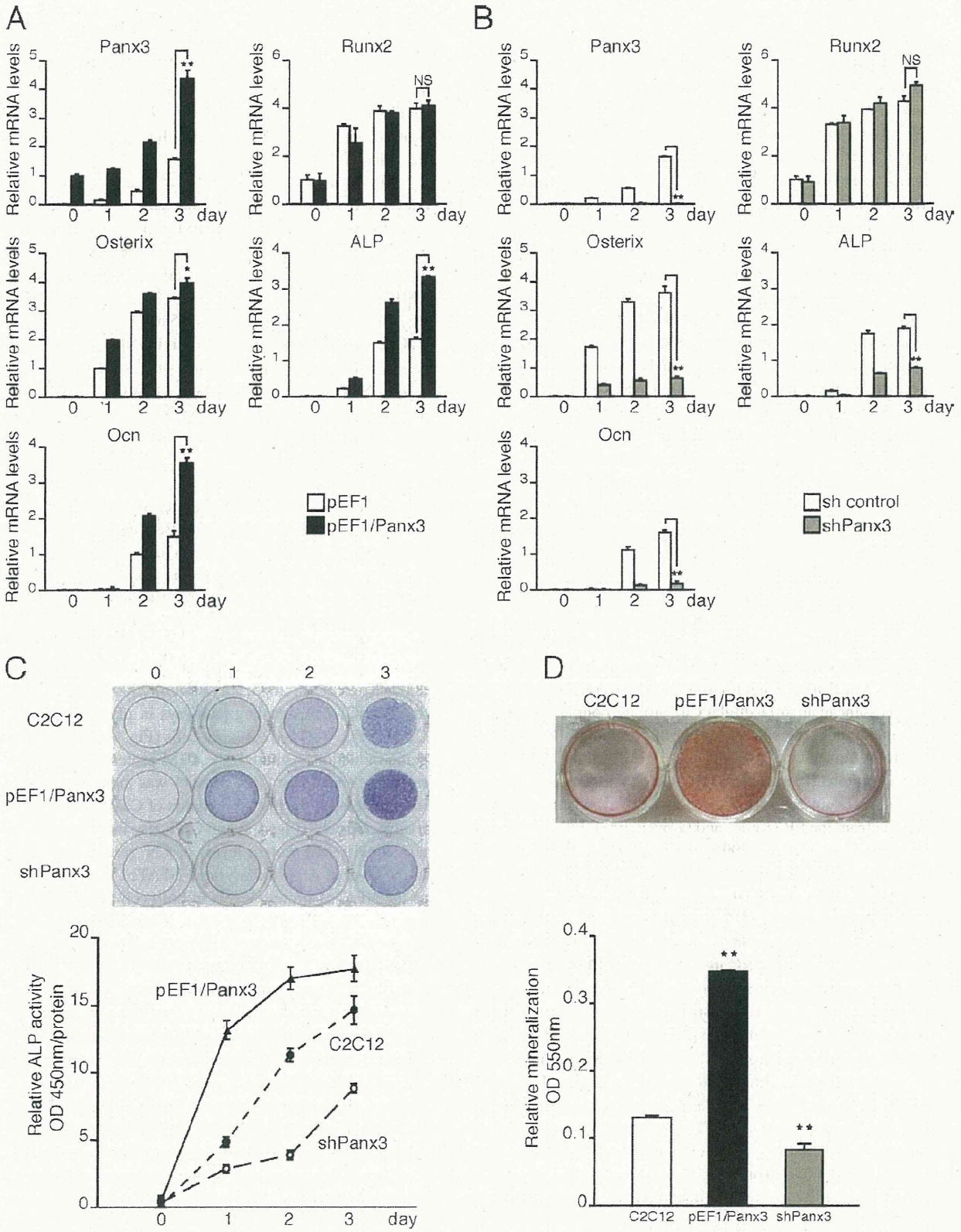

Figure 2. **Panx3 promotes osteoblast differentiation.** C2C12 cells were transiently transfected with a control pEF1 vector, pEF1/Panx3, a control sh vector, or a Panx3 shRNA vector, and these cells were cultured with BMP2 for various durations, as indicated. Total RNA was extracted each day for 4 d and mRNA levels were analyzed by quantitative RT-PCR. (A) Panx3 overexpression promoted the expression of osteoblast marker genes for osterix, ALP, and Ocn, except that the expression of Runx2 remained the same. (B) shPanx3 suppressed the induction of these genes, except for Runx2. (C) Panx3

Downloaded from jcb.rupress.org on May 6, 2012

Panx3 promotes metatarsal bone growth

Because Panx3 was expressed in the perichondrium/periosteum and osteoblasts, we analyzed Panx3 functions further with respect to ex vivo growth of the metatarsus. Metatarsal bones from newborn mice were cultured and infected with Panx3 expression adenovirus (AdPanx3). AdPanx3 promoted growth in the length and width of both cartilage and bone in metatarsus after 3 d in culture compared with the growth in the control adenovirus-infected metatarsus, as shown in videos and histology sections (Fig. 3 A, a; Fig. 3 B, a and b; and Videos 1 and 2). AdPanx3 infection increased not only the expression of Panx3, but also the expression of the osteoblast marker genes osterix, ALP, and Ocn (Fig. 3 C). To inhibit endogenous Panx3 activity, we used an inhibitory Panx3 peptide from the extracellular domain of Panx3, which blocked hemichannel activity and the release of ATP release (see Fig. 6), as described previously (Iwamoto et al., 2010). Addition of the Panx3 peptide to a metatarsus culture inhibited the growth in length and width compared with the growth without the peptide or growth in a culture with a control scrambled peptide (Figs. 3 A, b; Fig. 3 B, a and b; and Videos 3 and 4). The Panx3 peptide inhibited the expression of osteoblast marker genes (Fig. 3 C), which indicates that Panx3 regulates growth plate expansion.

Panx3 functions as an ER Ca^{2+} channel

Because the intracellular Ca^{2+} level ($[Ca2^{+}]_i$) plays an important role in osteoblast differentiation (Zayzafoon et al., 2005; Seo et al., 2009), we examined whether intracellular Ca^{2+} signaling is involved in Panx3-promoted osteoblast differentiation. The ER serves as the main intracellular Ca^{2+} storage compartment. In the ER membrane, the sarco/endoplasmic reticulum Ca^{2+}-ATPase (SERCA) takes up Ca^{2+} from the cytosol to the ER, whereas the ubiquitous IP3 receptors (IP3R1, -2, and -3), as well as the RyRs in certain cell types, serve as ER Ca^{2+} channels for Ca^{2+} release from the ER (Keller and Grover, 2000; Fill and Copello, 2002; Futatsugi et al., 2005). Extracellular ATP can bind to purinergic receptors (P2Rs) and subsequently activate downstream intracellular signaling cascades. These signaling pathways are known to promote IP3 production, thereby activating IP3R ER Ca^{2+} channels and increasing $[Ca^{2+}]_i$ (Solini et al., 2008). In C2C12 cells, all IP3Rs are expressed, with IP3R3 showing the highest expression level (Powell et al., 2001), whereas RyRs are not expressed (Fig. S1 C; Biswas et al., 1999). No significant change was observed in the expression levels of IP3Rs during osteogenic differentiation of C2C12 (Fig. S1 C). Because Panx3 was induced during differentiation of C2C12 and calvarial cells and was localized in the ER, Panx3 may function as an ER Ca^{2+} channel, thereby increasing $[Ca^{2+}]_i$ and subsequently promoting osteoblast differentiation. To explore Panx3 Ca^{2+} ER channel activity, Panx3 overexpressing C2C12 and calvarial cells were loaded with a UV-excitable intracellular Ca^{2+} indicator, Fura-2 AM, in Ca^{2+}-free media. The cells were then stimulated by ATP, and increases in the $[Ca^{2+}]_i$ level were measured over a time course and compared with $[Ca^{2+}]_i$ levels in control cells lacking Panx3 (Fig. 4 A, a and b). $[Ca^{2+}]_i$ was approximately twofold higher in Panx3-overexpressing C2C12 and calvarial cells than in control cells. This suggests that Panx3 may act as an ER Ca^{2+} channel.

To measure steady-state $[Ca^{2+}]_i$ levels during differentiation, C2C12 cells were cultured with BMP2, and $[Ca^{2+}]_i$ was analyzed without ATP stimulation (Fig. 4 A, c). The level of $[Ca^{2+}]_i$ in undifferentiated C2C12 cells was ~100 nM, a concentration typically observed in cells at rest. At 5 d after differentiation by BMP2, $[Ca^{2+}]_i$ was increased to ~180 nM, and this $[Ca^{2+}]_i$ increase was further enhanced to ~225 nM in Panx3-overexpressing C2C12 cells. Inhibition of differentiation by shPanx3 reduced $[Ca^{2+}]_i$. Collectively, these results suggest that Panx3 regulates $[Ca^{2+}]_i$. Similar $[Ca^{2+}]_i$ increases in calvarial cells were observed during osteogenic differentiation (Fig. S2 D).

Panx3 activates the CaM pathways for differentiation

Intracellular Ca^{2+} activates and affects many signaling pathways that modulate cell differentiation (Berridge et al., 2000a). Upon Ca^{2+} binding, CaM activates many downstream signaling molecules such as CaMKII and the phosphatase CN, and promotes osteoblast differentiation (Berridge et al., 2000b; Seo et al., 2009). NFATc1 is activated through dephosphorylation by CN and can promote expression of genes such as osterix, a key molecule involved in osteogenesis (Beals et al., 1997; Nakashima et al., 2002; Koga et al., 2005; Zayzafoon, 2006). We first examined the CaMKII–CN signaling pathways in pEF1/Panx3-transfected C2C12 (Fig. 4 B) and calvarial cells (Fig. 4 C) after short osteogenic induction. Although the CaM protein level remained the same, we found that CaM activity was induced, which resulted in an increase in the phosphorylation of CaMKII in pEF1/Panx3-transfected cells (Fig. 4, B and C). It also increased the phosphatase activity and protein levels of CN, resulting in an increase in the level of dephosphorylated NFATc1 (active form) as well as the NFATc1 protein levels in both cell types compared with control cells. The increase in NFATc1 protein levels is likely caused by the enhanced NFATc1 transcription levels in the CaMKII–c-fos pathway (Koga et al., 2005; Zayzafoon et al., 2005). In a subsequent experiment involving the inhibition of endogenous Panx3 expression, shPanx3- and shControl-transfected cells were cultured under induction conditions for 1 d to induce endogenous Panx3, and the activation of these factors was measured. Inhibition with shPanx3 reduced the phosphorylation levels of CaMKII and increased inactive phosphorylated NFATc1 levels in C2C12 cells and to a lesser extent in calvarial cells (Fig. 4, B and C). The effects of Panx3 on the CaM pathways were less prominent in calvarial cells than in C2C12 cells, likely because of differences in their transfection efficiency. pEF1/Paxn3 and

overexpression promoted ALP activity, whereas shPanx3 inhibited it. Representative ALP staining (top) and its quantitative data (bottom). C2C12 cells and pEF1/Panx3- and shPanx3-transfected C2C12 cells were cultured with BMP2 for 3 d. (D) Representative Alizarin red S staining (top) and its quantitative data (bottom) of C2C12 and pEF1/panx3- and shPanx3-transfected C2C12 cells cultured with BMP2 for 15 d. **, $P < 0.01$. Error bars represent the mean ± SD; $n = 3$.

Downloaded from jcb.rupress.org on May 6, 2012

Published June 20, 2011

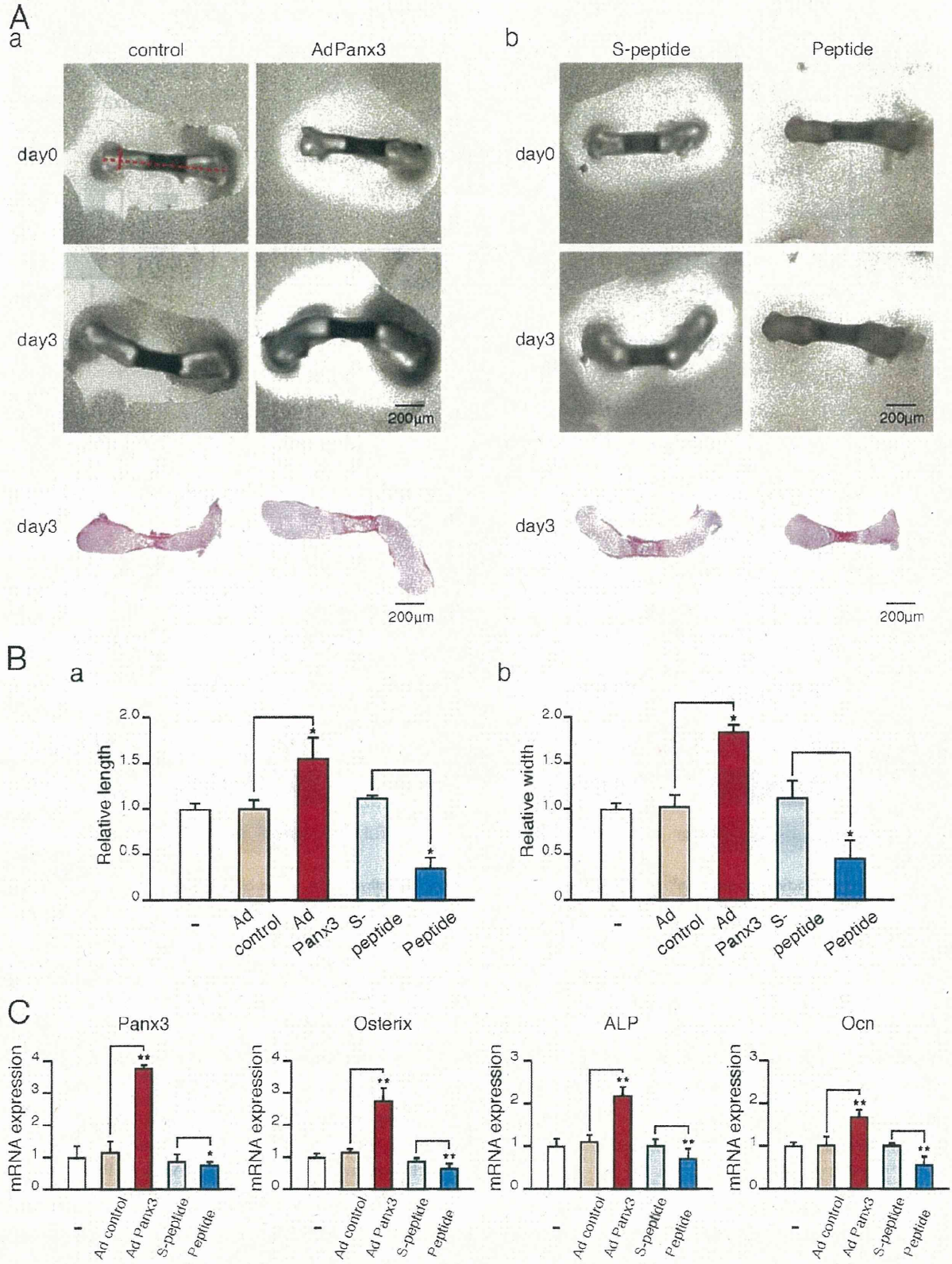

Figure 3. **Panx3 promotes the growth of metatarsus ex vivo.** (A) Live images of ex vivo metatarsal growth (top) and histology (bottom). (a) Newborn mouse metatarsal bones were cultured and infected with Panx3 adenovirus (AdPanx3) or control adenovirus. (b) Metatarsus cultures were incubated with the Panx3 peptide for 3 d. Metatarsal bone growth was measured by real-time imaging. AdPanx3 promoted metatarsal bone growth (a), whereas the Panx3 peptide inhibited it (b). (B) Relative change in metatarsal length (Ba) or width (Bb) after 3 d in culture compared with day 0. The bone length was

Downloaded from jcb.rupress.org on May 6, 2012

Published June 20, 2011

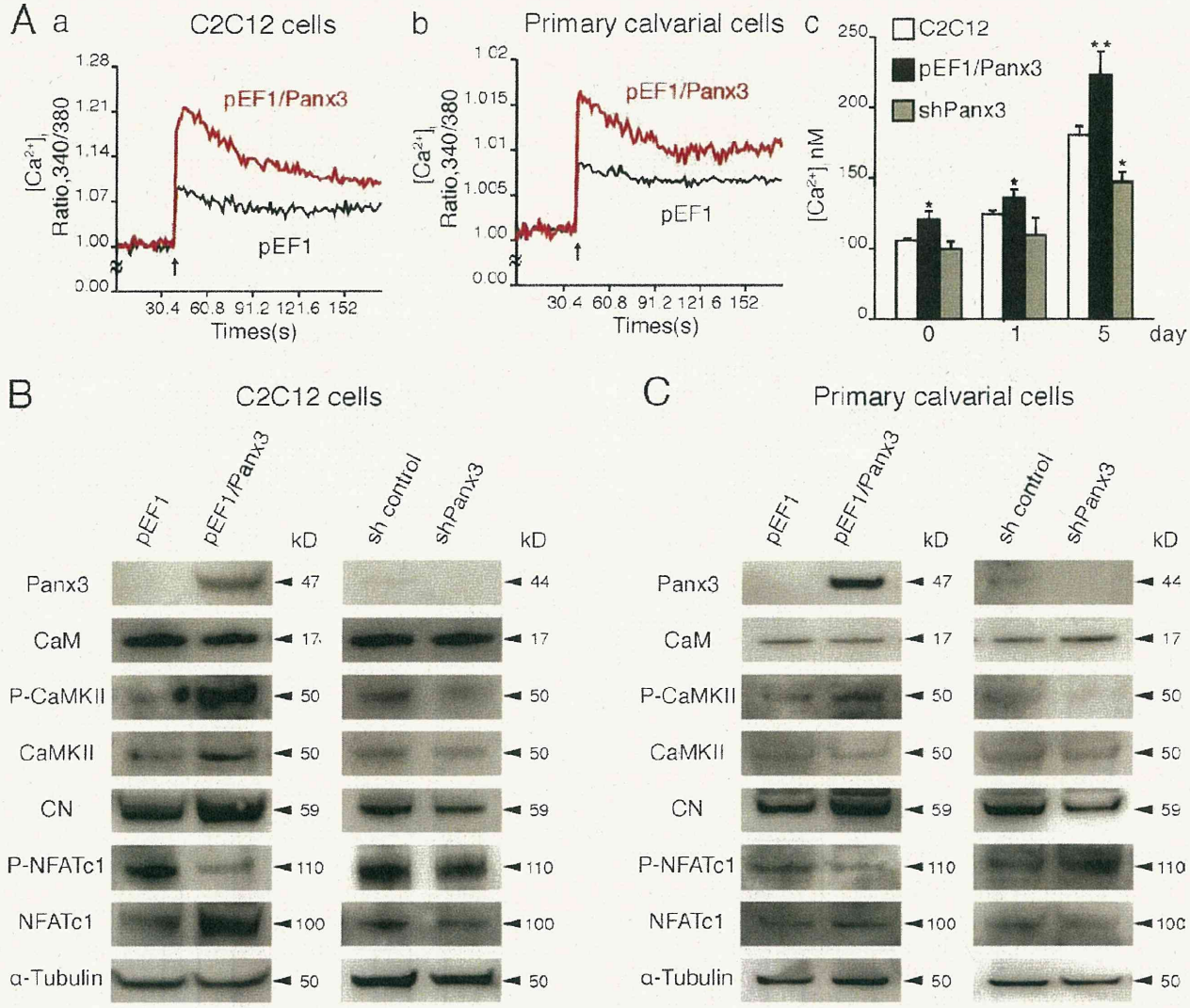

Figure 4. **Panx3 functions as an ER Ca^{2+} channel, and activates the CaM and Akt pathways.** (A, a and b) Panx3 ER Ca^{2+} channel. C2C12 cells stably transfected with pEF1 (black) or pEF1/Panx3 (red) expression vectors were analyzed for ATP-stimulated $[Ca^{2+}]_i$ in a time course (A, a). Primary calvarial cells were transiently transfected with pEF1 (black) or pEF1/Panx3 (red) expression vectors (A, b). The data shown are representative of at least four different experiments. (A, c) $[Ca^{2+}]_i$ levels during differentiation of C2C12 cells. Untransfected and stably transfected cells with pEF1/Panx3 or shPanx3 vectors were cultured with BMP2 at the indicated days. $[Ca^{2+}]_i$ levels in pEF1/Panx3-transfected cells were much higher than in C2C12 cells, whereas those in shPanx3 cells were lower. *, $P < 0.05$; **, $P < 0.01$. Error bars represent the mean ± SD, $n = 3$. (B and C) Panx3 activates the CaM/NFATc1 signaling pathways. C2C12 cells or primary calvarial cells were stably and transiently transfected with pEF1 and pEF1/Panx3 vectors, respectively, then incubated for 1 h with BMP2, and the levels of the signal molecules were analyzed by Western blotting. For shPanx3 inhibition experiments, stably transfected C2C12 cells or transiently transfected primary calvarial cells with sh control and shPanx3 RNA were cultured for 1 d in the presence of BMP2.

shPanx3 were transiently transfected into calvarial cells, whereas they were stably transfected into C2C12 cells.

Activation mechanism of Panx3 ER Ca^{2+} channel

Next, we determined whether any differences existed between the activation mechanisms of the Panx3 and IP3R ER Ca^{2+} channels by using inhibitors of the IP3R function (Vanden Abeele et al., 2006). In control undifferentiated C2C12 cells, 2-APB, an inhibitor of IP3-induced Ca^{2+} release (Maruyama et al., 1997), completely blocked Ca^{2+} release from the IP3R channel in control cells (Fig. 5 A, a). In Panx3-overexpressing undifferentiated C2C12 cells, 2-APB treatment resulted in a reduction in the $[Ca^{2+}]_i$ levels, which closely corresponded to the

measured from edge to edge (A, a, broken red line). The width was measured from side to side (A, a, red line). AdPanx3 promoted the growth of both length and width, whereas Panx3 peptide inhibited both. (C) Quantitative RT-PCR. Metatarsus cultures were incubated for 3 d with AdPanx3 or the Panx3 peptide. AdPanx3 promoted the expression of osteoblast marker genes, osterix, ALP, and Ocn. The Panx3 peptide inhibited this marker gene expression. *, $P < 0.05$; **, $P < 0.01$. Error bars represent the mean ± SD; $n = 3$.

Downloaded from jcb.rupress.org on May 6, 2012

Published June 20, 2011

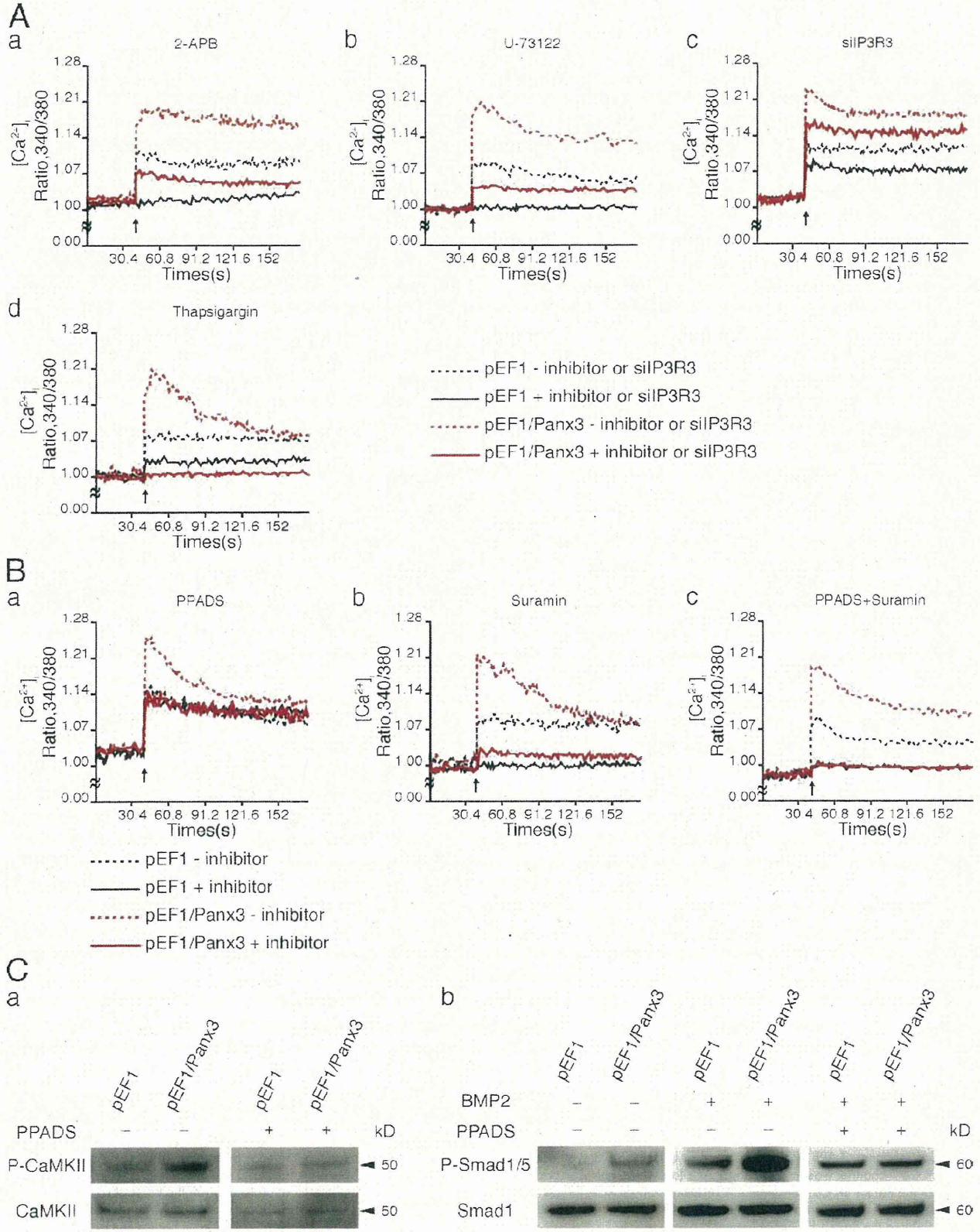

Figure 5. **Panx3 ER Ca^{2+} channel activation and its downstream signaling.** C2C12 cells stably transfected with pEF1 or pEF1/Panx3 expression vectors were analyzed for ATP-stimulated $[Ca^{2+}]_i$. Inhibitors were added to the cell culture for 30 min before ATP stimulation. In inhibition to endogenous IP3R3 expression, $[Ca^{2+}]_i$ was analyzed after 3 d of transfection of C2C12 cells with siRNA for IP3R3. (A) Panx3 ER Ca^{2+} channel independent of the IP3R ER

Downloaded from jcb.rupress.org on May 6, 2012

$[Ca^{2+}]_i$ levels in control cells (Fig. 5 A, a). This indicates that 2-APB inhibited the IP3R ER Ca^{2+} channel, but not the Panx3 ER Ca^{2+} channel. In control cells, U-73122, a selective inhibitor of PLC, which catalyzes DAG and IP3 synthesis (Bleasdale et al., 1990), completely blocked the IP3R Ca^{2+} channel (Fig. 5 A, b); however, it only partially inhibited the Panx3 ER Ca^{2+} channel (Fig. 5 A, b). Inhibition of endogenous IP3R3 expression by siRNA reduced the IP3R Ca^{2+} channel but not the Panx3 ER Ca^{2+} channel (Fig. 5 A, c). Thapsigargin, a highly selective inhibitor of the SERCA ER Ca^{2+} pumps responsible for loading Ca^{2+} stores (Inesi and Sagara, 1992), partially inhibited IP3R-mediated Ca^{2+} release from the ER in control cells (Fig. 5 A, d), whereas it completely blocked Ca^{2+} release from the ER in Panx3-overexpressing cells (Fig. 5 A, c). This suggests that the Panx3 ER Ca^{2+} channel continuously released Ca^{2+} from the ER after thapsigargin treatment. Therefore, the activation mechanism for the Panx3 ER Ca^{2+} channel appears to be different from that of the IP3R.

Because Panx3 and IP3R ER Ca^{2+} channels are both activated by external ATP, we tested the differences in ATP receptors involved in the activation of these channels. ATP receptors (purinergic receptors, P2Rs) consist of two subtypes, the ligand-gated cation channels (P2Xs) and the G protein–coupled receptors (P2Ys; Burnstock and Knight, 2004). During osteoblast differentiation, a series of P2X and P2Y subtypes are expressed (Hoebertz et al., 2000; Orriss et al., 2006; Panupinthu et al., 2008). To examine whether specific subtypes of P2Rs are required for the activation of the Panx3 ER Ca^{2+} channel, the P2R antagonists pyridoxal-phosphate-6-azophenyl-2′,4′-disulfonate (PPADS) and suramin were tested for their effects on ATP-stimulated changes in $[Ca^{2+}]_i$ in Panx3-overexpressing and control cells (Fig. 5 B). PPADS inhibited Panx3 ER Ca^{2+} channel activity in Panx3-overexpressing C2C12 cells (Fig. 5 B, a), whereas it did not inhibit the IP3R Ca^{2+} channel in control cells (Fig. 5 B, a). Suramin completely inhibited the IP3R Ca^{2+} channel in control cells (Fig. 5 B, b), and partially inhibited the Panx3 ER channel in Panx3-overexpressing cells (Fig. 5 B, b). A combination of PPADS and suramin completely inhibited both Panx3 and IP3R ER channels (Fig. 5 B, c). These results indicated that the Panx3 ER Ca^{2+} channel is activated through PPADS-sensitive P2Rs that are distinct from the IP3R channel.

Because PPADS specifically inhibited the Panx3 ER Ca^{2+} channel, we tested whether it would also inhibit Panx3-mediated CaM activation. For these experiments, we treated control and Panx3 overexpressing C2C12 cells with BMP-2 for 1 h and then analyzed the phosphorylation of CaMKII and Smad1/5, both of which are targets of CaM (Fig. 5 C; Wicks et al., 2000; Pardali et al., 2005). PPADS inhibited phosphorylation of CaMKII induced by Panx3 overexpression (Fig. 5 C, a). Without BMP2 treatment, Panx3 overexpression resulted in activation of Smad1/5 (Fig. 5 C, b, left). BMP2 induced phosphorylation of Smad1/5 in control cells, and Panx3 overexpression further increased phosphorylation levels of Smad1/5 (Fig. 5 C, b, middle), whereas this stimulation was blocked by PPADS (Fig. 5 C, b, right). These results suggest that the activation of specific P2Rs may be involved in Panx3-mediated signaling for osteoblast differentiation through CaMKII and Smad1/5 pathways.

Panx3 activates the Akt pathway

In addition to P2R-mediated activation of the PLC–PIP2–IP3–IP3R pathway, P2Rs also activate PI3K signaling. Because Akt downstream from PI3K is crucial for osteoblast differentiation (Fujita et al., 2004; Mukherjee and Rotwein, 2009), we explored the involvement of Akt in Panx3-promoted osteoblast differentiation. We found that Panx3 overexpression increased phosphorylation of Akt and Akt-downstream MDM2, and promoted the degradation of p53 in both C2C12 and calvarial cells (Fig. 6 A, a and b). p53 is a negative regulator of osteogenesis (Lengner et al., 2006) and inhibits Runx2 and osterix expression (Lian et al., 2006). Akt-mediated MDM2 phosphorylation leads to p53 ubiquitination (Ogawara et al., 2002). Our results indicate that Panx3 expression activates Akt and promotes p53 degradation through MDM2 activation.

An Akt inhibitor reduced the expression of osterix mRNA in control and pEF1/Panx3-transfected C2C12 cells. The dominant-negative Akt vector (Akt DN) also inhibited osterix expression, whereas the activated Akt vector increased the expression (Fig. 6 B, a). Similar results were found for ALP expression (Fig. 6 B, b). These results suggest that Panx3 promotes osteoblast differentiation in part through the Akt pathway.

Akt activates the Panx3 ER Ca^{2+} channel

We next examined the involvement of Akt in the activation of a Panx3 ER Ca^{2+} channel. We found that the Akt inhibitor abolished ATP-stimulated Panx3 ER Ca^{2+} channel activity in Panx3-overexpressing C2C12 cells (Fig. 7 A, a). The remaining Ca^{2+} released from the ER was likely through the IP3R ER Ca^{2+} channel, which showed an activity level similar to that in control cells. The Akt inhibitor did not inhibit the IP3R ER Ca^{2+} channel in control cells. Akt DN also inhibited the ATP-stimulated Panx3 ER Ca^{2+} release, but not IP3R ER Ca^{2+} release (Fig. 7 A, b). In contrast, activated constitutively active Akt (Akt CA) increased the activity of the Panx3 ER Ca^{2+} channel, but not the activity of the IP3R ER Ca^{2+} channel (Fig. 7 A, c). In control cells, neither

Ca^{2+} channel. 2-APB (IP3R inhibitor; a) or U-73122 (IP3 synthesis inhibitor; b) completely inhibited Ca^{2+} release from the IP3R ER Ca^{2+} channel. The Panx3 ER Ca^{2+} channel was inhibited by 2-APB (a), whereas it was partially inhibited by U-73122 (b). siRNA for IP3R3 inhibited the IP3R3 ER Ca^{2+} channel, but not the Panx3 ER Ca^{2+} channel (c). Thapsigargin (SERCA ER Ca^{2+} pump inhibitor) completely inhibited Ca^{2+} release from the ER in pEF1/Panx3-transfected cells, whereas it partially inhibited it in pEF1-transfected cells (d). The data shown are representative of at least three different experiments. (B) PPADS inhibited the Panx3 ER Ca^{2+} channel but not the IP3R ER Ca^{2+} channel (a). Suramin completely inhibited the IP3R ER Ca^{2+} channel but partially inhibited the Panx3 ER Ca^{2+} channel (b). A combination of PPADS and suramin blocked both ER Ca^{2+} channels (c). Arrows indicate the time of ATP addition. The data shown are representative of at least three different experiments. (C) PPADS inhibition of CaM downstream signaling. Stably transfected C2C12 cells with pEF1 and pEF1/Panx3 vectors were incubated for 1 h with BMP2, with or without PPADS, and levels of phosphorylation of CaMKII (a) and Smad1/5 (b) phosphorylation were analyzed by Western blotting. The left panel in b indicates Smad1/5 phosphorylation levels in cells without BMP2 and PPADS. In the middle and right panels of b, cells were induced by BMP2.

Downloaded from jcb.rupress.org on May 6, 2012

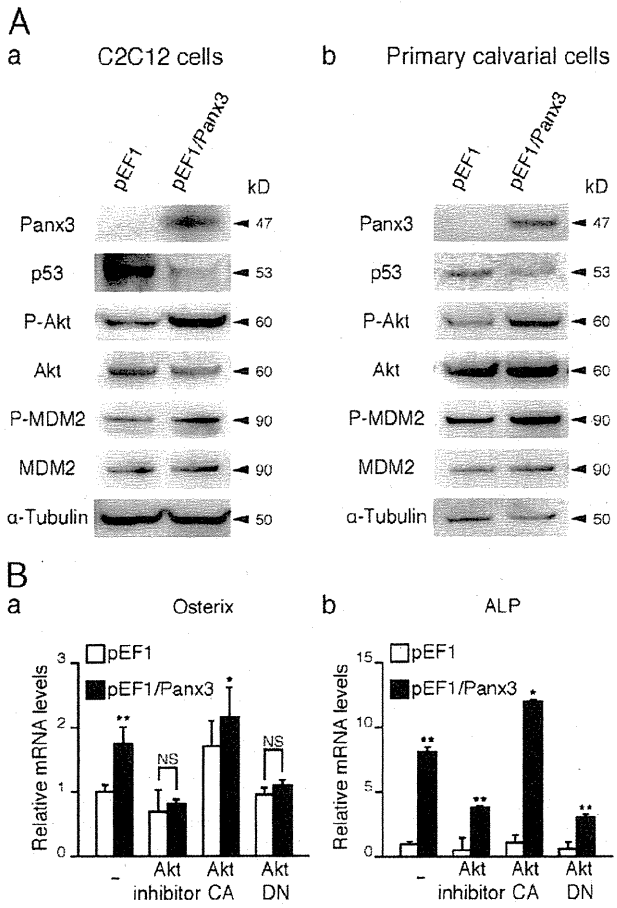

Figure 6. **Panx3 activates the Akt pathway.** (A, a and b) Panx3 activates Akt signaling. Stably transfected C2C12 cells or transiently transfected primary calvarial cells with pEF1 and pEF1/Panx3 vectors were incubated for 1 h with BMP2, and levels of signal molecules were analyzed by Western blotting. Panx3 expression increased phosphorylation of Akt and MDM2 and promoted p53 degradation. (B) Akt inhibition reduced Panx3-promoted expression of osterix (a) and ALP expression (b). The transfected cells were cultured with BMP2 for 3 d, and the expression of osterix and ALP was analyzed by real-time PCR. The Akt inhibitor and Akt DN inhibited the expression of Panx3-mediated induction of these genes, whereas Akt CA increased the expression levels in control and Panx3-overexpressing cells. *, $P < 0.05$; **, $P < 0.01$. Error bars indicate the mean ± SD; $n = 3$.

Akt vector affected the IP3R ER Ca^{2+} channel (Fig. 7 A, b and c). LY294002, an inhibitor of PI3K, inhibited both Panx3 and IP3R ER channels (Fig. 7 A, d). The reason for this was that PI3K activates Akt as well as the IP3 synthesis pathway (Carpenter and Cantley, 1996). These results suggest that ATP-stimulated activation of the Panx3 ER Ca^{2+} channel is mediated through a PI3K–Akt activation that is distinct from the IP3-dependent activation of IP3R ER Ca^{2+} channels.

To further confirm the Akt-mediated activation of the Panx3 ER Ca^{2+} channel, the $[Ca^{2+}]_i$ concentration was measured without ATP stimulation (Fig. 7 B). The steady-state $[Ca^{2+}]_i$ concentration in Panx3-overexpressing C2C12 cells was ~140 nM, which was higher than that of control cells (90 nM). The activated Akt enhanced the $[Ca^{2+}]_i$ concentration in Panx3-overexpressing C2C12 cells by about twofold (280 nM) compared with that in cells without the Akt vector. Akt DN reduced the steady-state $[Ca^{2+}]_i$ concentration in Panx3-overexpressing C2C12 cells to a level similar to that seen in the control cells. These results indicated that the Panx3 ER Ca^{2+} channel is regulated by Akt signaling, and that its mechanism is independent of IP3R activity.

We further examined whether Akt-mediated Panx3 ER Ca^{2+} channel activation regulates the CaM–CaMKII–NFATc1 signaling pathways (Fig. 7 C). Panx3-overexpressing C2C12 cells were transfected with the Akt CA or Akt DN vector and were treated with BMP2 for 1 h. Western blotting analysis showed that Akt CA increased phosphorylation of CaMKII (P-CaMKII) and activation of NFATc1 (reduced P-NFATc1), whereas Akt DN inhibited CaMKII and NFATc1 activation (Fig. 7 C). These results support the notion that the Akt signaling pathway regulates the Panx3 ER Ca^{2+} channel.

Panx3 releases intracellular ATP through its hemichannel activity

The activation of P2Rs may be caused in part by binding of ATP released from cells through Panx3 hemichannel activity. To test this possibility, we first analyzed the intracellular ATP levels in control and Panx3-overexpressing C2C12 cells by fluorescence imaging using confocal microscopy (Fig. 8 A, a). The cells containing caged luciferin were illuminated by a flash of two-photon light, which photolyzed the caged luciferin, allowing the uncaged luciferin to bind to intracellular ATP and resulting in an increase in fluorescence emissions. The fluorescence intensity at 5 and 15 s after photolysis was much higher (red) in control C2C12 cells than in Panx3-overexpressing cells, which suggests that Panx3 expression reduced intracellular ATP levels. To analyze ATP release, control and Panx3-overexpressing C2C12 and calvarial cells were incubated in the presence of luciferin for 2 min, and the fluorescence intensity was measured (Fig. 8 A, b and c). The extracellular ATP level was approximately twofold higher in Panx3-expressing cells than in control cells. Similar results were obtained when the cells were treated with KGlu to depolarize the cell membrane, except that the level of ATP release was much higher. Addition of anti-Panx3 antibody, but not IgG, to the cell culture assay inhibited Panx3-mediated ATP release (Fig. 8 B, a). To test whether this inhibition was specific to Panx3, we used the inhibitory Panx3 peptide from the extracellular domain of Panx3, which had been used as an antigen for the Panx3 antibody (Iwamoto et al., 2010). The peptide, but not a scrambled peptide, blocked the inhibitory activity of the antibody for the ATP release in a dose-dependent manner (Fig. 8 B, a). In addition, the Panx3 peptide alone showed inhibitory activity for the ATP release, as described previously in chondrogenic ATDC5 cells (Iwamoto et al., 2010). Under differentiation conditions, suppression of endogenous Panx3 by shRNA inhibited ATP release in C2C12 cells (Fig. 8 B, b). These results indicated that Panx3 caused the release of intracellular ATP into the extracellular space though the hemichannel.

To test the effects of the Panx3 hemichannel on osteoblast differentiation, control and Panx3-overexpressing C2C12 cells were induced to differentiate by a 2-d treatment with BMP2, in the presence or absence of the anti-Panx3 antibody, and mRNA levels for osterix and ALP were analyzed (Fig. 8 C). The Panx3 antibody inhibited the induction of osterix and ALP expression

Downloaded from jcb.rupress.org on May 6, 2012

Published June 20, 2011

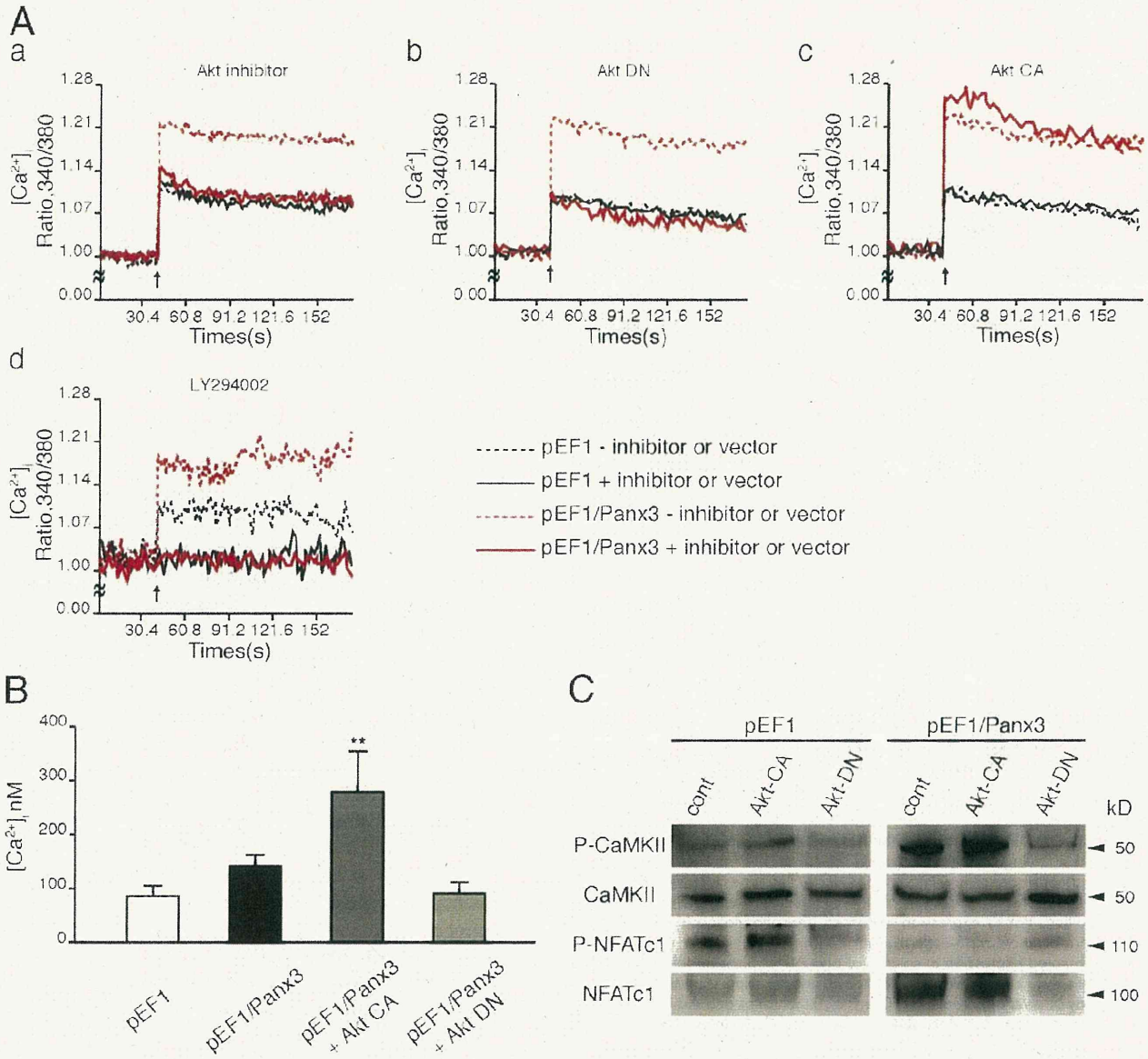

Figure 7. **Activation of Panx3 ER Ca^{2+} channel by PI3K–Akt signaling.** (A) pEF1- or pEF1/Panx3-transfected C2C12 cells were incubated with the Akt inhibitor (a), or transfected with the dominant-negative Akt (Akt DN; b), the activated Akt (Akt CA) vector (c), or LY294002 (PI3K inhibitor; d). $[Ca^{2+}]_i$ was measured by the fluorescence intensity ratio of Fura-2 (F_{340nm}/F_{380nm}) in each condition. The Akt inhibitor blocked the Panx3 ER Ca^{2+} channel (a). Akt DN inhibited the Panx3 ER Ca^{2+} channel, not the IP3R ER channel (b). Akt CA promoted the Panx3 ER Ca^{2+} channel, not the IP3R ER channel (c). LY294002 inhibited Ca^{2+} release from both Panx3 and IP3R ER Ca^{2+} channels (d). Arrows indicate the time of ATP addition. The data shown are representative of at least three different experiments. (B) The $[Ca^{2+}]_i$ level was increased by Akt activation. The basal levels of $[Ca^{2+}]_i$ in Panx3-overexpressing C2C12 (pEF1/Panx3) cells are higher than in control vector–transfected (pEF1) cells. Akt CA increased $[Ca^{2+}]_i$ in pEF1/Panx3 cells, whereas Akt DN reduced $[Ca^{2+}]_i$ to similar levels in control cells. (C) The transfected cells were induced by BMP2 for 1 h, and phosphorylation of CaMKII and NFATc1 was analyzed by Western blotting. Akt increased CaMKII and NFATc1 phosphorylation levels in control cells, and Panx3 overexpression further enhanced its activation. Akt DN inhibited these activations to the levels in control cells. *, $P < 0.05$; **, $P < 0.01$. Error bars indicate the mean ± SD; $n = 3$.

in both control and Panx3-overexpressing cells. Because the antibody and peptide blocked the Panx3 hemichannel activity, these results suggest that the Panx3 hemichannel plays a critical role in osteoblast differentiation.

Panx3 gap junction function during osteoblast differentiation

An increase in $[Ca^{2+}]_i$ in one cell can be transmitted to neighboring cells, resulting in Ca^{2+} waves that spread within cell networks. This Ca^{2+} wave propagation is mediated by gap junctions and promotes cell–cell communication for cellular processes and differentiation (Barbe et al., 2006). Therefore, we examined Panx3 gap junction activity in C2C12 cells and its effect on osteoblast differentiation (Fig. 9). First, Ca^{2+} wave propagation in Panx3-overexpressing C2C12 cells was analyzed and compared with that in control cells. The cells were loaded with a photosensitive caged form of Ca^{2+} and Ca^{2+}-sensitive Fluo-4. While performing live-cell Ca^{2+} imaging, a

Downloaded from jcb.rupress.org on May 6, 2012

Published June 20, 2011

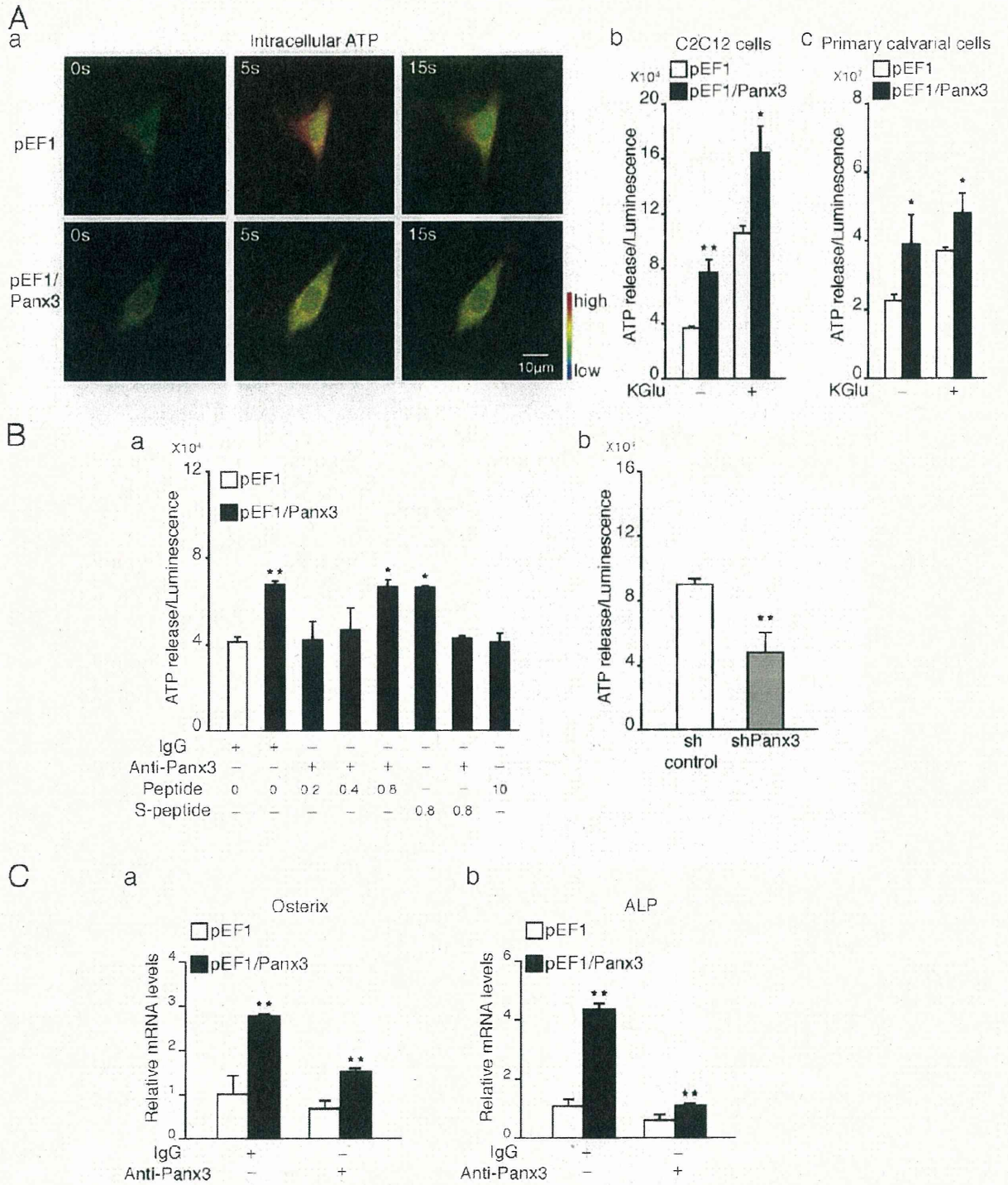

Figure 8. **Panx3 hemichannel releases intracellular ATP and promotes differentiation.** (A) Imaging of intracellular ATP levels in pEF1- or pEF1/Panx3-transfected C2C12 cells. Cells were incubated with the caged luciferin, and then exposed to a flash of UV light for photolysis to convert active luciferin. Fluorescence excitation images (red) caused by luciferin–ATP interactions at 5 s and 15 s after a UV flash were shown. Higher red fluorescence images were observed in control pEF1-transfected cells compared with Panx3-overexpressing cells, which indicates that Panx3 overexpression reduced intracellular ATP levels. (A, b and c) Measurement of ATP release. The transfected C2C12 cells or primary calvarial cells were treated with or without KGlu for 2 min, and then ATP released into the media was measured. (B) Inhibition of ATP release. The transfected cells were incubated with Panx3 antibody or Panx3 peptide for 30 min, and ATP release was measured. The Panx3 antibody (1.5 μg/ml) inhibited ATP release in pEF1/Panx3-transfected cells (a). This inhibition was blocked by various concentrations of the Panx3 peptide. The Panx3 peptide also inhibited the ATP release (a). Control sh- or shPanx3-transfected cells were cultured with BMP2 for 2 d, and ATP release was measured. ATP release was reduced in shPanx3-transfected cells compared with control sh-transfected cells (b). (C) Inhibition of osterix (a) and ALP (b) expression by the anti-Panx3 antibody. *, $P < 0.05$; **, $P < 0.01$. Error bars represent the mean ± SD; $n = 3$.

Downloaded from jcb.rupress.org on May 6, 2012

Published June 20, 2011

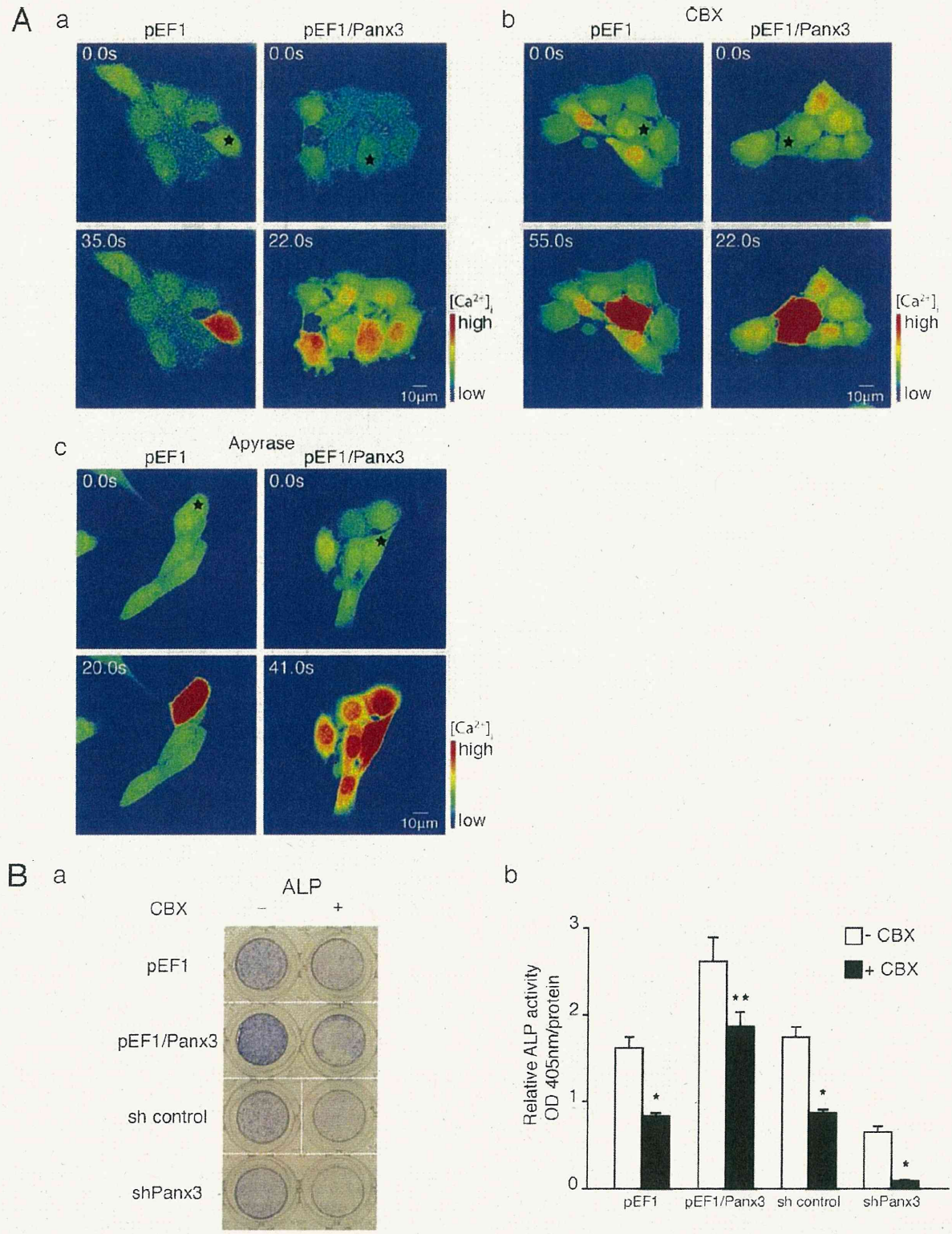

Figure 9. **Panx3 functions as a gap junction.** (A) Real-time imaging of Ca^{2+} wave propagation. The Ca^{2+} wave was measured in cells loaded with Fluo-4 and NP-EGTA (caged Ca^{2+}) by starting photolysis of NP-EGTA in a single cell using a flash of UV light. (a) pEF1/Panx3-transfected cells, but not pEF1-transfected cells, propagated Ca^{2+} waves to neighboring cells. (b) Inhibition of the Ca^{2+} wave propagation by CBX (gap junction inhibitor). (c) Apyrase, ATP receptor antagonist, did not inhibit Ca^{2+} propagation in pEF1/Panx3-transfected cells. (B) CBX inhibited C2C12 cell differentiation. (a) ALP staining. (b) Quantitative data from the ALP staining. CBX inhibited osteoblast differentiation in pEF1/Panx3-transfected cells (a and b). *, $P < 0.05$; **, $P < 0.01$. Error bars represent the mean ± SD; $n = 3$.

Downloaded from jcb.rupress.org on May 6, 2012

Published June 20, 2011

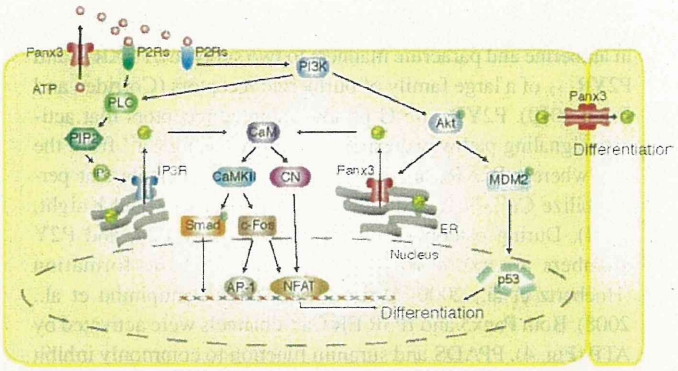

Figure 10. **Panx3 pathways in osteoblast differentiation.** The Panx3 hemichannel releases intracellular ATP. The released ATP binds to purinoreceptors (P2Rs) in its own cell and/or neighboring cells, and activates the PI3K–Akt pathway. Akt then activates the Panx3 ER Ca^{2+} channel to increase $[Ca^{2+}]_i$ levels, which leads to activation of the CaM–CaMKII pathway. The ATP also activates the PLC–PIP2–IP3R ER Ca^{2+} channel pathway, which is distinct from that of the Panx3 ER Ca^{2+} channel. The Akt activation also phosphorylates MDM2, which induces degradation of p53, an inhibitor for osteogenic differentiation, and promotes differentiation. CaM also activates CN, which dephosphorylates inactive phosphorylated NFAT in cytosol. Dephosphorylated NFATc1 enters the nucleus and binds to the promoter regions of differentiation genes such as osterix and ALP. Activated CaMKII also increases c-fos and NFAT expression, and activation of Ap-1 and Smad1/5. Panx3 gap junction activity promotes Ca^{2+} wave propagation between adjacent cells for differentiation.

single cell within a cell network was subjected to two-photon photolysis. The uncaged Ca^{2+} fluctuations were analyzed by live-cell fluorescence confocal microscopy (Fig. 9 A, a; and Videos 5 and 6). We also observed similar Ca^{2+} wave propagation in Panx3-overexpressing calvarial cells (unpublished data). In Panx3-overexpressing cells, Ca^{2+} waves were propagated into neighboring cells (red in high Ca^{2+}), whereas in control cells lacking Panx3, the Ca^{2+} fluctuations were restricted to the single uncaged cell. This Ca^{2+} wave propagation was inhibited by the gap junction inhibitor carbenoxolone (CBX; Fig. 9 A, b; and Videos 7 and 8). Because CBX may disrupt the cell membrane and affect activation of P2 receptors, thereby inhibiting the Ca^{2+} wave, apyrase (an ATP receptor antagonist) was added to the Ca^{2+} wave assay at a concentration, which inhibited Panx3-mediated activation of Akt signaling (Fig. S3). We found that apyrase did not inhibit the Ca^{2+} wave, which suggests that Panx3 gap junction mediates Ca^{2+} wave propagation (Fig. 9 A, c; and Videos 9 and 10). To test the effect of Panx3-mediated gap junction activity on C2C12 cell differentiation, Panx3-overexpressing and control cells were induced to differentiate by BMP2 treatment in the presence of CBX, and ALP activity was measured (Fig. 9 B). Panx3 overexpression promoted ALP activity, as shown in Fig. 2, but CBX inhibited this ALP activation. Similarly, Panx3 shRNA inhibited ALP induction, as shown in Fig. 2, and CBX further inhibited ALP activity. These results indicated that Panx3 can function as a gap junction and propagate Ca^{2+} waves from cell to cell, and that this activity also promotes osteoblast differentiation.

Discussion

In our present study, we demonstrated for the first time that Panx3 regulates osteoblast differentiation through its multiple functions as a hemichannel, an ER Ca^{2+} channel, and a gap junction, as illustrated in Fig. 10. All three Panx3 activities are associated with and involved in osteoblast differentiation. We showed that Panx3 is induced during osteogenic differentiation and is localized in the plasma membrane, and that it functions as the hemichannel that releases ATP into the extracellular space. The ATP released from the cells binds to purinergic receptors (P2Rs) in the plasma membrane in an autocrine and paracrine manner, and thereby activates P2R–PI3K–Akt signaling for the Panx3 channel and P2R–PLC–PIP2–IP3 for the IP3R channel. Akt-mediated Panx3 ER Ca^{2+} channel activation induces Ca^{2+} release from the ER into the cytosol, which subsequently activates CaM signaling pathways, including CaMKII–Smad, CaMKII–c-Fos, and CN–NFATc. The Akt activation also increases p53 degradation through activation of MDM2. The activation of these pathways promotes differentiation. In addition, the increased $[Ca^{2+}]_i$ level that originated in cells because of the hemichannel in turn propagates its wave into surrounding cells through a Panx3 gap junction, subsequently promoting Ca^{2+} signaling among cell populations for differentiation. Because blocking of the Panx3 hemichannel inhibits osteoblast differentiation, this hemichannel activation may be the first step in Panx3-mediated differentiation processes.

Ca^{2+} is one of the most important second messengers and regulates many cellular processes (Berridge et al., 2000b), and the CaM pathway is critical for osteoblast differentiation (Zayzafoon, 2006). However, the mechanism for controlling $[Ca^{2+}]_i$ during osteoblast differentiation is not yet clear. We found that Panx3 functions as a Ca^{2+} channel in the ER, through which it regulates $[Ca^{2+}]_i$. C2C12 and calvarial cells express IP3Rs. Both Panx3 and IP3Rs function as ER Ca^{2+} channels; however, their activation mechanisms are different. We found that the Panx3 ER Ca^{2+} channel was activated through Akt signaling (Fig. 7 A), distinct from IP3-mediated activation of ubiquitous IP3R ER Ca^{2+} channels (Mikoshiba, 2007). In addition, siRNA for IP3R3 and 2-APB, which is an inhibitor of IP3R-mediated Ca^{2+} release, inhibited IP3R ER Ca^{2+} channel activity, but did not inhibit the Panx3 channel (Fig. 5 A). The role of IP3Rs in osteogenic differentiation is also not yet clear. The inhibition of endogenous Panx3 by shRNA resulted in substantial inhibition of osteogenic differentiation in C2C12 cells, despite IP3R expression, whereas the inhibition of IP3Rs by siRNA and 2-APB showed limited inhibition of C2C12 cell differentiation (unpublished data). In addition, mice lacking either IP3R2 or IP3R3 were viable and had no obvious abnormalities. Mice lacking both IP3R2 and IP3R3 were born with a normal appearance but began losing body weight after weaning because of defects in exocrine secretion (Futatsugi et al., 2005). Both receptors may function as ER Ca^{2+} channels with distinct activation mechanisms during osteogenic differentiation. Because the Panx3 hemichannel likely triggers activation of these Panx3 and IP3R ER Ca^{2+} channels, Panx3 may play a major role upstream of IP3Rs in osteogenic differentiation.

Downloaded from jcb.rupress.org on May 6, 2012

Extracellular ATP modulates cellular functions by binding in autocrine and paracrine manners to two subtypes, $P2XR_{1-7}$ and $P2YR_{1-12}$, of a large family of purinergic receptors (Corriden and Insel, 2010). P2YRs are G protein–coupled receptors that activate signaling pathways responsible for releasing Ca^{2+} from the ER, whereas P2XRs are nonselective cation channels that permeabilize Ca^{2+}, Na^{+}, and other cations (Burnstock and Knight, 2004). During osteoblast differentiation, many P2X and P2Y members are expressed and implicated in bone formation (Hoebertz et al., 2000; Orriss et al., 2006; Panupinthu et al., 2008). Both Panx3 and IP3R ER Ca^{2+} channels were activated by ATP (Fig. 4). PPADS and suramin function to commonly inhibit some P2Ys and P2XRs (e.g., P2X1, P2X3, and P2Y6); however, they also inhibit specifically (e.g., PPADS for P2Y1 and P2Y4; suramin for P2X2, P2X5, and P2Y2; P2 receptors; Burnstock, 2007). Panx3 ER Ca^{2+} channels, but not IP3R ER Ca^{2+} channels, were inhibited by PPADS (Boyer et al., 1994; Ziganshin et al., 1994), whereas suramin inhibited both channels (Fig. 5 B). These results suggest that the Panx3 and IP3R ER Ca^{2+} channels may be regulated through different purinergic receptors. The ATP-induced $[Ca^{2+}]_i$ experiments were performed in cell culture without external Ca^{2+} in the medium to measure $[Ca^{2+}]_i$ released from the ER. However, in vivo, external Ca^{2+} may also contribute to an increase in $[Ca^{2+}]_i$ through the ATP-P2X cation channels. Indeed, P2X7 knockout mice displayed reduced periosteal bone formation and response to mechanical loading (Ke et al., 2003; Li et al., 2005).

Panx3 expression increased phosphorylation of Akt (Fig. 6 A). Akt signaling is required for osteoblast differentiation, bone formation, and prevention of osteoblast apoptosis (Kawamura et al., 2007; Mukherjee and Rotwein, 2009). One of the Akt target pathways is the MDM2/p53 signaling pathway (Lengner et al., 2006; Wang et al., 2006). Panx3 expression promoted phosphorylation of MDM2 and enhanced the degradation of the p53 protein (Fig. 6 A). These results indicate that Panx3-promoted osteogenic differentiation occurs in part due to reduction of the p53 level through enhancement of the Akt–MDM2–p53 pathway (Fig. 10). We found that Panx3 also stimulated phosphorylation of Smad1/5 (Fig. 5 C). Previous studies have shown that CaM–CaMKII activates Smad1/5 (Scherer and Graff, 2000), and therefore, Panx3 ER Ca^{2+} channel/CaM–CaMKII signaling activates Smad1/5. The anti-Panx3 antibody and PPADS inhibited the Panx3-promoted Smad1/5 activation, which suggests that the Panx3 hemichannel and P2Rs are involved in these processes.

Panx1 and Panx2 were expressed in C2C12 and primary calvarial cells at a very low level and were not induced at all during osteogenic differentiation of these cells (unpublished data). Therefore, Panx3 is the major pannexin protein expressed during osteoblast differentiation. Among the connexin gap junction proteins, Cx43 is the most highly expressed in osteoblasts (Civitelli et al., 1993; Su et al., 1997; Gramsch et al., 2001; Jiang et al., 2007), and is implicated in osteoblast differentiation and mineralization (Lecanda et al., 2000; Stains and Civitelli, 2005; Chung et al., 2006; Inose et al., 2009). Cx43 knockout mice showed cranial abnormalities and delayed ossification, whereas axial and appendicular elements were normal at birth (Lecanda et al., 2000). Mice with conditional Cx43 deletion in osteoblasts displayed a normal appearance at birth but developed a low bone density osteopenia phenotype with age (Chung et al., 2006). Panx3 overexpression in differentiated C2C12 cells promoted Cx43 expression, whereas suppression of endogenous Panx3 by Panx3 shRNA inhibited Cx43 expression (unpublished data). These results suggest that Panx3 and Cx43 may play distinct roles in osteogenic differentiation.

In summary, we have provided evidence that Panx3 acts as a multifunctional protein that promotes osteoblast differentiation by regulating Akt and Ca^{2+} signaling through its hemichannel, ER channel, and gap junction activities.

Materials and methods

Reagents

Rabbit anti-Panx3 antibody, inhibitory Panx3 and scrambled peptides, Panx3 expression vector (pEF1/Panx3) and control vector (pEF1), shRNA vector for Panx3 (shPanx3), and control vector (sh control) have been described previously (Iwamoto et al., 2010). In brief, the pEF1/Panx3 vector was constructed by cloning the coding sequence of mouse Panx3 cDNA into the pEF1/V5-His vector (Invitrogen). The shPanx3 vector containing the 3′ untranslated region of Panx3 (5′-GGCAGGGTAGAACAATTTA-3′) in a pSM2 vector was obtained from Thermo Fisher Scientific. A rabbit polyclonal antibody to a peptide (amino acid residues HHTQDKAGQYKVK-SLWPH) from the mouse Panx3 protein was generated and purified with a peptide affinity column. This Panx3 peptide was also used for inhibition experiments. A peptide with a scrambled sequence (WHTKYQVGLDPQH-KASHK) of the Panx3 peptide was used as a control. Control adenovirus (Ad-Cont) and Panx3 expression adenovirus (Ad-Panx3) were prepared and purified by Welgen, Inc. Akt CA and Akt DN vectors were obtained from Addgene. Antibodies for P-Rb, CaM, CaMKII, P-CaMKII, CN, p53, Akt, p-Akt, Smad1, and P-Smad1/5 were obtained from Cell Signaling Technology; Rb, P-NFATc1, and MDM2 were from Santa Cruz Biotechnology, Inc.; NFATc1 was from BD; α-tubulin from Sigma-Aldrich; Ocn from Biomedical Technology; and calnexin from Thermo Fisher Scientific. 2-APB, U-73122, thapsigargin, PPADS, suramin, CBX, and apyrase were obtained from Sigma-Aldrich; Akt inhibitor was from EMD; LY294002 and Fura-2AM were from Invitrogen; BMP2 was from Humanzyme; and iQ SYBR Green Supermix was from Bio-Rad Laboratories. HRP-conjugated goat anti–mouse and goat anti–rabbit IgG were obtained from United States Biological.

Cell culture

Mouse C2C12 cells were grown in DME (Invitrogen) containing 10% FBS (HyClone) at 37°C under 5% CO_2. For osteoblast differentiation, cells (~90% confluence) were transiently or stably transfected with pEF1/Panx3, control vector, Panx3 shRNA, or sh control vector and cultured in the presence of 300 ng/ml BMP2 (Humanzyme) and 2% FBS. The media were replaced every 3 d. Primary calvarial cells were prepared from calvaria of newborn mice as described previously (Matsunobu et al., 2009). Calvaria were digested six times for 10 min with 0.1% collagenase type 1 (Worthington Biochemical Corp.) and 0.2% dispase II (Roche) in PBS. The last two fractions were centrifuged at 1,500 rpm for 5 min, resuspended in culture medium consisting of α-minimum essential medium (Invitrogen) with 10% FBS (HyClone), 100 U/ml of penicillin, and 100 μg/ml of streptomycin. Primary calvarial cells were transiently transfected with Nucleofector (Lonza). For the differentiation assay, primary calvarial cells were induced by the addition of 50 μg/ml ascorbic acid (Sigma-Aldrich) and 5 mM β-glycerophosphate (Sigma-Aldrich).

Immunostaining

Growth plates of newborn mice were fixed overnight in 4% paraformaldehyde and dehydrated before they were embedded in paraffin. After deparaffinization and rehydration, sections were digested with pepsin (Biocare Medical), blocked by Rodent block (Biocare Medical), and then reacted with primary antibodies for 2 h at room temperature. In cell culture, C2C12 cells were blocked by Power block (Biocare Medical) and reacted with primary antibodies under the same condition as described in the Cell culture section. Primary antibodies were detected by Alexa Fluor 488 (Invitrogen)- or Cy-3 (Jackson ImmunoResearch Laboratories)-conjugated

Downloaded from jcb.rupress.org on May 6, 2012

secondary antibodies. Nuclear staining was performed with Hoechst dye (Sigma-Aldrich). Analysis was performed on an inverted confocal microscope (LSM 510) and a fluorescence microscope (Axiovert 200; both from Carl Zeiss). Colocalization was analyzed by MetaMorph (Molecular Devices).

RT-PCR

Total RNA was extracted using the Nuclear Extraction System Quick-Gene-810 and HC kit S (Fujifilm). Total RNA (1 µg) was used for reverse transcription to generate cDNA, which was used as a template for PCRs with gene-specific primers (Table S1), as described previously (Iwamoto et al., 2010). The cDNA was amplified with an initial denaturation at 95°C for 3 min; then 95°C for 30 s, 60°C for 30 s, and 72°C for 30 s for 30 cycles; and then amplified with a final elongation step at 72°C for 5 min before being separated on agarose gels. Real-time PCR amplification was performed with iQ SYBR Green Supermix (Bio-Rad Laboratories) and a Chromo4 thermocycler (Bio-Rad Laboratories). Real-time PCR was performed for 40 cycles at 95°C for 1 min, 60°C for 1 min, and 72°C for 1 min. Gene expression was normalized to the housekeeping gene Hprt.

ATP flux

ATP flux was determined by luminometry, as described previously (Iwamoto et al., 2010). To open the pannexin channels, the cells were depolarized by incubation in KGlu solution (140 mM KGlu, 10 mM KCl, and 5.0 mM TES, pH 7.5) for 10 min. The supernatant was collected and assayed with luciferase/luciferin (Promega). The luminescence was measured using a multimode plate reader, Mithras LB 940 (Berthold). For inhibition by the Panx3-antibody, the cells were incubated with 1.5 ng/ml affinity-purified antibody or control IgG for 30 min before assay.

Western blot analysis

The cells were washed three times with PBS containing 1 mM sodium vanadate (Na_3VO_4), then solubilized in 100 µl of lysis buffer (10 mM Tris-HCl, pH 7.4, 150 mM NaCl, 10 mM $MgCl_2$, 0.5% Nonidet P-40, 1 mM phenylmethylsulfonyl fluoride, and 20 U/ml aprotinin). Lysed cells were centrifuged at 14,000 rpm for 30 min, and the protein concentration of each sample was measured with Micro-BCA Assay Reagent (Thermo Fisher Scientific). A 10 µg sample of each protein was electrophoresed in 4–12% SDS-polyacrylamide gel (Invitrogen) and transferred onto a polyvinylidene difluoride membrane using iBlot (Invitrogen). The membranes were immunoblotted with antibodies using standard protocols.

ALP assay

C2C12 cells and primary calvarial cells were plated into 12- or 96-well culture plates and grown to 100% confluence. The cells were then induced to differentiate into osteoblasts by addition of 300 ng/ml BMP2. ALP activity was measured in cell layers using a *p*-nitrophenyl phosphate substrate and an incubation temperature of 37°C, or was determined by the tartrate-resistant acid phosphatase (TRACP) & ALP double-stain kit (Takara Bio Inc.). The protein concentration was determined by the BCA protein assay method (Thermo Fisher Scientific).

Alizarin red S staining

C2C12 cells were fixed with 60% isopropanol and stained with 1% (wt/vol) Alizarin red S (Sigma-Aldrich). Calcium deposition was quantified as previously described (Mukherjee and Rotwein, 2009). In brief, the cultures were extracted from the Alizarin red S stain with 10% cetylpyridinium chloride (Sigma-Aldrich), and the OD was measured at 550 nm.

Ex vivo metatarsal bone culture

Metatarsal bones were isolated from newborn C57BL/6 mice and were cultured in DME containing 0.5% bovine serum albumin, 50 µg/ml ascorbic acid (Sigma-Aldrich), and 1 mM β-glycerol phosphate (Sigma-Aldrich) at 37°C in a humidified atmosphere of 5% CO_2, as described previously (Mukherjee and Rotwein, 2009). One day after starting the culture, the metatarsal bones were infected with Ad-Cont or Ad-Panx3 (1×10^9 PFU/ml) for 3 d. For the peptide inhibition assay, Panx3 antigen peptide or a scramble peptide (100 µg/ml) was added to the metatarsal cultures and incubated for 3 d. Live images were captured with a camera (Infinity2; Lumenera) attached to a microscope (Axiovert 25; Karl Zeiss). Images were analyzed and adjusted using MetaMorph (Molecular Devices) and National Institutes of Health ImageJ software. Metatarsals were fixed in 4% paraformaldehyde overnight at 4°C and stored in 70% ethanol. Bones were embedded in paraffin blocks and sectioned. Sections were stained with hematoxylin and eosin. Images were captured with microscope camera (AxioCam; Carl Zeiss) attached to a microscope (Axiovert 135; Carl Zeiss).

$[Ca^{2+}]_i$ measurements

C2C12 cells were grown in a 96-well plate for 3 d and then loaded with 5 µM Fura-2AM (Invitrogen) prepared in HBSS for 45 min at 37°C in 5% CO_2. After 3 d of transfection, transiently transfected primary calvarial cells were loaded at the same condition as the C2C12 cells. The Ca^{2+} transients were recorded as the 340/380 nm ratio (R) of the resulting 510-nm emissions using a plate reader (Mithras LB 940; Berthold Technologies). For the stimulation, 200 µM of ATP was automatically injected into cells by the Mithras 940. For inhibition experiments, cells were incubated for 30 min before analysis with one of the following inhibitors: 5 M U-73122 for IP3 synthesis inhibition, 100 µM 2-APB for blocking IP3R, 0.5 µM thapsigargin for SERCA ER Ca^{2+} pump inactivation, 100 µM PPADS, and 300 µM suramin for P2Rs inhibition; 5 µM Akt inhibitor; and 100 µM LY294002 for PI3K inhibition. The C2C12 cells that had been stably transfected with either pEF1/Panx3 or control vector were then transiently transfected with siIP3R-3 (Thermo Fisher Scientific). After 3 d of transfection, $[Ca^{2+}]_i$ was measured. The $[Ca^{2+}]_i$ levels were calculated as described previously (Grynkiewicz et al., 1985) using the equation $[Ca^{2+}]_i = K_d (R - R_{min})/(R_{max} - R)(F^{380}{}_{max}/F^{380}{}_{min})$, where R_{min} is the ratio at zero Ca^{2+}, R_{max} is the ratio when Fura-2 is completely saturated with Ca^{2+}, $F^{380}{}_{min}$ is the fluorescence at 380 nm for zero Ca^{2+}, and $F^{380}{}_{max}$ is the fluorescence at saturating Ca^{2+} and K_d = 224 nM.

Imaging of single-cell intracellular ATP concentrations and Ca^{2+} wave propagation

For the imaging of single-cell intracellular ATP levels, cells attached to glass-bottomed dishes (MatTek Corporation) were loaded with 25 µM of caged D-luciferin AM (Invitrogen) in HBSS containing 10 mM Hepes for 20 min at room temperature, followed by washing. The cells were then incubated with KGlu solution for 10 min. For Ca^{2+} wave propagation, cells seeded in a glass bottom dish were incubated in HBSS containing 4 µM of the Ca^{2+} indicator Fluo-4 AM, 10 µM pluronic F-127 (Invitrogen), 0.1% OxyFluor (Oxyrase), and 2.5 µM caged reagent NP-EGTA AM (Invitrogen) for 30 min at room temperature, followed by washing and incubation with Ca^{2+}-free HBSS. Both luciferin AM and Fluo-AM were imaged using a microscope (LSM 510 NLO META) equipped with A-Plan-Apochromat 63× (1.4 NA) objective lenses (all from Carl Zeiss). A 488 nm argon laser line was used for excitation. Cells were imaged every 1 s for ~1 min after the uncaging step. D-Luciferin AM and NP-EGTA AM were uncaged using a two-photon laser set at 730 nm. A nucleus-sized region of interest was used for uncaging within single cells using the Zen software's bleach function (Carl Zeiss). To block the gap junction channels, cells were incubated with 25 µM CBX. To inhibit ATP receptors, cells were incubated with 20 U apyrase.

Focal microscopy images were obtained using a two-photon confocal microscope. 488 nm argon, 543 nm HeNe1, and 633 nm HeNe2 lasers were used to excite Cy2, Cy3, and Cy5 fluorophores, respectively. The pinholes for each laser line were aligned for optimal confocality. For DAPI illumination, the two-photon laser was tuned to 730 nm and used at ~3–8% power.

Data analysis

Each experiment was repeated several times. The data were analyzed by Prism 5 software. Statistical differences between two groups of data were analyzed with a Student's *t* test. A one-way ANOVA was used for the quantification of Alizarin red S staining. $P < 0.05$ was considered statistically significant.

Online supplemental material

Fig. S1 shows Panx3 expression levels in the pEF1/Panx3- and shPanx3-transfected C2C12 cells, and the protein expression levels for Panx3, IP3R3, and RyR3 in undifferentiated and differentiated C2C12 cells. Fig. S2 shows the effects of Panx3 expression or shPanx3 inhibition on calvarial cell differentiation and an increase in $[Ca^{2+}]$ levels during differentiation of calvarial cells. Fig. S3 shows the inhibition of Akt activation by apyrase in C2C12 cells transfected with pEF1/Panx3. Videos 1–4 show imaging of ex vivo metatarsal growth by infection with Panx3 adenovirus (AdPanx3) or treatment with the inhibitory Panx3 peptide. Videos 5–8 show imaging of the Ca^{2+} wave propagation in the pEF1/Panx3 transfected C2C12 cells with and without CBX, and Videos 9 and 10 show no inhibitory effects of apyrase on the Ca^{2+} wave propagation. Table S1 shows the primers used for semi-quantitative and quantitative RT-PCR. Online supplemental material is available at http://www.jcb.org/cgi/content/full/jcb.201101050/DC1.

Downloaded from jcb.rupress.org on May 6, 2012

Published June 20, 2011

We thank Patricia Forcinito, Tomoya Matsunobu, Akira Futatsugi, and Indu Ambudkar for their suggestions.

This work was supported by the Intramural Program of the National Institute of Dental and Craniofacial Research, National Institutes of Health (to Y. Yamada), and grant-in-aids (20791583 to T. Iwamoto) and (20679006 to S. Fukumoto) from the Ministry of Education, Science, and Culture of Japan. M. Ishikawa was supported in part by a Fellowship from the Japan Society for the Promotion of Science.

Submitted: 12 January 2011
Accepted: 25 May 2011

References

Baranova, A., D. Ivanov, N. Petrash, A. Pestova, M. Skoblov, I. Kelmanson, D. Shagin, S. Nazarenko, E. Geraymovych, O. Litvin, et al. 2004. The mammalian pannexin family is homologous to the invertebrate innexin gap junction proteins. *Genomics*. 83:706–716. doi:10.1016/j.ygeno.2003.09.025

Barbe, M.T., H. Monyer, and R. Bruzzone. 2006. Cell-cell communication beyond connexins: the pannexin channels. *Physiology (Bethesda)*. 21:103–114.

Beals, C.R., N.A. Clipstone, S.N. Ho, and G.R. Crabtree. 1997. Nuclear localization of NF-ATc by a calcineurin-dependent, cyclosporin-sensitive intramolecular interaction. *Genes Dev.* 11:824–834. doi:10.1101/gad.11.7.824

Bennett, M.V., and V.K. Verselis. 1992. Biophysics of gap junctions. *Semin. Cell Biol.* 3:29–47. doi:10.1016/S1043-4682(10)80006-6

Berridge, M.J., P. Lipp, and M.D. Bootman. 2000a. Signal transduction. The calcium entry pas de deux. *Science*. 287:1604–1605. doi:10.1126/science.287.5458.1604

Berridge, M.J., P. Lipp, and M.D. Bootman. 2000b. The versatility and universality of calcium signalling. *Nat. Rev. Mol. Cell Biol.* 1:11–21. doi:10.1038/35036035

Biswas, G., O.A. Adebanjo, B.D. Freedman, H.K. Anandatheerthavarada, C. Vijayasarathy, M. Zaidi, M. Kotlikoff, and N.G. Avadhani. 1999. Retrograde Ca2+ signaling in C2C12 skeletal myocytes in response to mitochondrial genetic and metabolic stress: a novel mode of inter-organelle crosstalk. *EMBO J.* 18:522–533. doi:10.1093/emboj/18.3.522

Bleasdale, J.E., N.R. Thakur, R.S. Gremban, G.L. Bundy, F.A. Fitzpatrick, R.J. Smith, and S. Bunting. 1990. Selective inhibition of receptor-coupled phospholipase C-dependent processes in human platelets and polymorphonuclear neutrophils. *J. Pharmacol. Exp. Ther.* 255:756–768.

Boyer, J.L., I.E. Zohn, K.A. Jacobson, and T.K. Harden. 1994. Differential effects of P2-purinoceptor antagonists on phospholipase C- and adenylyl cyclase-coupled P2Y-purinoceptors. *Br. J. Pharmacol.* 113:614–620.

Bruzzone, S., L. Guida, E. Zocchi, L. Franco, and A. De Flora. 2001. Connexin 43 hemi channels mediate Ca2+-regulated transmembrane NAD+ fluxes in intact cells. *FASEB J.* 15:10–12.

Bruzzone, R., S.G. Hormuzdi, M.T. Barbe, A. Herb, and H. Monyer. 2003. Pannexins, a family of gap junction proteins expressed in brain. *Proc. Natl. Acad. Sci. USA*. 100:13644–13649. doi:10.1073/pnas.2233464100

Burnstock, G., and G.E. Knight. 2004. Cellular distribution and functions of P2 receptor subtypes in different systems. *Int. Rev. Cytol.* 240:31–304. doi:10.1016/S0074-7696(04)40002-3

Burnstock, G. 2007. Purine and pyrimidine receptors. *Cell. Mol. Life Sci.* 64:1471–1483. doi:10.1007/s00018-007-6497-0

Carpenter, C.L., and L.C. Cantley. 1996. Phosphoinositide kinases. *Curr. Opin. Cell Biol.* 8:153–158. doi:10.1016/S0955-0674(96)80060-3

Celetti, S.J., K.N. Cowan, S. Penuela, Q. Shao, J. Churko, and D.W. Laird. 2010. Implications of pannexin 1 and pannexin 3 for keratinocyte differentiation. *J. Cell Sci.* 123:1363–1372. doi:10.1242/jcs.056093

Chung, D.J., C.H. Castro, M. Watkins, J.P. Stains, M.Y. Chung, V.L. Szejnfeld, K. Willecke, M. Theis, and R. Civitelli. 2006. Low peak bone mass and attenuated anabolic response to parathyroid hormone in mice with an osteoblast-specific deletion of connexin43. *J. Cell Sci.* 119:4187–4198. doi:10.1242/jcs.03162

Civitelli, R., E.C. Beyer, P.M. Warlow, A.J. Robertson, S.T. Geist, and T.H. Steinberg. 1993. Connexin43 mediates direct intercellular communication in human osteoblastic cell networks. *J. Clin. Invest.* 91:1888–1896. doi:10.1172/JCI116406

Corriden, R., and P.A. Insel. 2010. Basal release of ATP: an autocrine-paracrine mechanism for cell regulation. *Sci. Signal.* 3:re1. doi:10.1126/scisignal.3104re1

D'hondt, C., R. Ponsaerts, H. De Smedt, G. Bultynck, and B. Himpens. 2009. Pannexins, distant relatives of the connexin family with specific cellular functions? *Bioessays*. 31:953–974. doi:10.1002/bies.200800236

Fill, M., and J.A. Copello. 2002. Ryanodine receptor calcium release channels. *Physiol. Rev.* 82:893–922.

Fujita, T., Y. Azuma, R. Fukuyama, Y. Hattori, C. Yoshida, M. Koida, K. Ogita, and T. Komori. 2004. Runx2 induces osteoblast and chondrocyte differentiation and enhances their migration by coupling with PI3K-Akt signaling. *J. Cell Biol.* 166:85–95. doi:10.1083/jcb.200401138

Futatsugi, A., T. Nakamura, M.K. Yamada, E. Ebisui, K. Nakamura, K. Uchida, T. Kitaguchi, H. Takahashi-Iwanaga, T. Noda, J. Aruga, and K. Mikoshiba. 2005. IP3 receptor types 2 and 3 mediate exocrine secretion underlying energy metabolism. *Science*. 309:2232–2234. doi:10.1126/science.1114110

Gramsch, B., H.D. Gabriel, M. Wiemann, R. Grümmer, E. Winterhager, D. Bingmann, and K. Schirrmacher. 2001. Enhancement of connexin 43 expression increases proliferation and differentiation of an osteoblast-like cell line. *Exp. Cell Res.* 264:397–407. doi:10.1006/excr.2000.5145

Grynkiewicz, G., M. Poenie, and R.Y. Tsien. 1985. A new generation of Ca2+ indicators with greatly improved fluorescence properties. *J. Biol. Chem.* 260:3440–3450.

Hoebertz, A., A. Townsend-Nicholson, R. Glass, G. Burnstock, and T.R. Arnett. 2000. Expression of P2 receptors in bone and cultured bone cells. *Bone*. 27:503–510. doi:10.1016/S8756-3282(00)00351-3

Inesi, G., and Y. Sagara. 1992. Thapsigargin, a high affinity and global inhibitor of intracellular Ca2+ transport ATPases. *Arch. Biochem. Biophys.* 298:313–317. doi:10.1016/0003-9861(92)90416-T

Inose, H., H. Ochi, A. Kimura, K. Fujita, R. Xu, S. Sato, M. Iwasaki, S. Sunamura, Y. Takeuchi, S. Fukumoto, et al. 2009. A microRNA regulatory mechanism of osteoblast differentiation. *Proc. Natl. Acad. Sci. USA*. 106:20794–20799. doi:10.1073/pnas.0909311106

Iwamoto, T., T. Nakamura, A. Doyle, M. Ishikawa, S. de Vega, S. Fukumoto, and Y. Yamada. 2010. Pannexin 3 regulates intracellular ATP/cAMP levels and promotes chondrocyte differentiation. *J. Biol. Chem.* 285:18948–18958. doi:10.1074/jbc.M110.127027

Jiang, J.X., A.J. Siller-Jackson, and S. Burra. 2007. Roles of gap junctions and hemichannels in bone cell functions and in signal transmission of mechanical stress. *Front. Biosci.* 12:1450–1462. doi:10.2741/2159

Kawamura, N., F. Kugimiya, Y. Oshima, S. Ohba, T. Ikeda, T. Saito, Y. Shinoda, Y. Kawasaki, N. Ogata, K. Hoshi, et al. 2007. Akt1 in osteoblasts and osteoclasts controls bone remodeling. *PLoS ONE*. 2:e1058. doi:10.1371/journal.pone.0001058

Ke, H.Z., H. Qi, A.F. Weidema, Q. Zhang, N. Panupinthu, D.T. Crawford, W.A. Grasser, V.M. Paralkar, M. Li, L.P. Audoly, et al. 2003. Deletion of the P2X7 nucleotide receptor reveals its regulatory roles in bone formation and resorption. *Mol. Endocrinol.* 17:1356–1367. doi:10.1210/me.2003-0021

Keller, D., and A.K. Grover. 2000. Nerve growth factor treatment alters Ca2+ pump levels in PC12 cells. *Neuroreport*. 11:65–68. doi:10.1097/00001756-200001170-00013

Koga, T., Y. Matsui, M. Asagiri, T. Kodama, B. de Crombrugghe, K. Nakashima, and H. Takayanagi. 2005. NFAT and Osterix cooperatively regulate bone formation. *Nat. Med.* 11:880–885. doi:10.1038/nm1270

Laird, D.W. 2006. Life cycle of connexins in health and disease. *Biochem. J.* 394:527–543. doi:10.1042/BJ20051922

Lecanda, F., P.M. Warlow, S. Sheikh, F. Furlan, T.H. Steinberg, and R. Civitelli. 2000. Connexin43 deficiency causes delayed ossification, craniofacial abnormalities, and osteoblast dysfunction. *J. Cell Biol.* 151:931–944. doi:10.1083/jcb.151.4.931

Lengner, C.J., H.A. Steinman, J. Gagnon, T.W. Smith, J.E. Henderson, B.E. Kream, G.S. Stein, J.B. Lian, and S.N. Jones. 2006. Osteoblast differentiation and skeletal development are regulated by Mdm2-p53 signaling. *J. Cell Biol.* 172:909–921. doi:10.1083/jcb.200508130

Li, J., D. Liu, H.Z. Ke, R.L. Duncan, and C.H. Turner. 2005. The P2X7 nucleotide receptor mediates skeletal mechanotransduction. *J. Biol. Chem.* 280:42952–42959. doi:10.1074/jbc.M506415200

Lian, J.B., G.S. Stein, A. Javed, A.J. van Wijnen, J.L. Stein, M. Montecino, M.Q. Hassan, T. Gaur, C.J. Lengner, and D.W. Young. 2006. Networks and hubs for the transcriptional control of osteoblastogenesis. *Rev. Endocr. Metab. Disord.* 7:1–16. doi:10.1007/s11154-006-9001-5

Maruyama, T., T. Kanaji, S. Nakade, T. Kanno, and K. Mikoshiba. 1997. 2APB, 2-aminoethoxydiphenyl borate, a membrane-penetrable modulator of Ins(1,4,5)P3-induced Ca2+ release. *J. Biochem.* 122:498–505.

Matsunobu, T., K. Torigoe, M. Ishikawa, S. de Vega, A.B. Kulkarni, Y. Iwamoto, and Y. Yamada. 2009. Critical roles of the TGF-beta type I receptor ALK5 in perichondrial formation and function, cartilage integrity, and osteoblast differentiation during growth plate development. *Dev. Biol.* 332:325–338. doi:10.1016/j.ydbio.2009.06.002

Mikoshiba, K. 2007. IP3 receptor/Ca2+ channel: from discovery to new signaling concepts. *J. Neurochem.* 102:1426–1446. doi:10.1111/j.1471-4159.2007.04825.x

Downloaded from jcb.rupress.org on May 6, 2012

Mukherjee, A., and P. Rotwein. 2009. Akt promotes BMP2-mediated osteoblast differentiation and bone development. *J. Cell Sci.* 122:716–726. doi:10.1242/jcs.042770

Nakashima, K., X. Zhou, G. Kunkel, Z. Zhang, J.M. Deng, R.R. Behringer, and B. de Crombrugghe. 2002. The novel zinc finger-containing transcription factor osterix is required for osteoblast differentiation and bone formation. *Cell.* 108:17–29. doi:10.1016/S0092-8674(01)00622-5

Ogawara, Y., S. Kishishita, T. Obata, Y. Isazawa, T. Suzuki, K. Tanaka, N. Masuyama, and Y. Gotoh. 2002. Akt enhances Mdm2-mediated ubiquitination and degradation of p53. *J. Biol. Chem.* 277:21843–21850. doi:10.1074/jbc.M109745200

Orriss, I.R., G.E. Knight, S. Ranasinghe, G. Burnstock, and T.R. Arnett. 2006. Osteoblast responses to nucleotides increase during differentiation. *Bone.* 39:300–309. doi:10.1016/j.bone.2006.02.063

Panchin, Y., I. Kelmanson, M. Matz, K. Lukyanov, N. Usman, and S. Lukyanov. 2000. A ubiquitous family of putative gap junction molecules. *Curr. Biol.* 10:R473–R474. doi:10.1016/S0960-9822(00)00576-5

Panupinthu, N., J.T. Rogers, L. Zhao, L.P. Solano-Flores, F. Possmayer, S.M. Sims, and S.J. Dixon. 2008. P2X7 receptors on osteoblasts couple to production of lysophosphatidic acid: a signaling axis promoting osteogenesis. *J. Cell Biol.* 181:859–871. doi:10.1083/jcb.200708037

Pardali, K., M. Kowanetz, C.H. Heldin, and A. Moustakas. 2005. Smad pathway-specific transcriptional regulation of the cell cycle inhibitor p21(WAF1/Cip1). *J. Cell. Physiol.* 204:260–272. doi:10.1002/jcp.20304

Penuela, S., R. Bhalla, X.Q. Gong, K.N. Cowan, S.J. Celetti, B.J. Cowan, D. Bai, Q. Shao, and D.W. Laird. 2007. Pannexin 1 and pannexin 3 are glycoproteins that exhibit many distinct characteristics from the connexin family of gap junction proteins. *J. Cell Sci.* 120:3772–3783. doi:10.1242/jcs.009514

Penuela, S., S.J. Celetti, R. Bhalla, Q. Shao, and D.W. Laird. 2008. Diverse subcellular distribution profiles of pannexin 1 and pannexin 3. *Cell Commun. Adhes.* 15:133–142. doi:10.1080/15419060802014115

Powell, J.A., M.A. Carrasco, D.S. Adams, B. Drouet, J. Rios, M. Müller, M. Estrada, and E. Jaimovich. 2001. IP(3) receptor function and localization in myotubes: an unexplored Ca(2+) signaling pathway in skeletal muscle. *J. Cell Sci.* 114:3673–3683.

Scemes, E., S.O. Suadicani, G. Dahl, and D.C. Spray. 2007. Connexin and pannexin mediated cell-cell communication. *Neuron Glia Biol.* 3:199–208. doi:10.1017/S1740925X08000069

Scherer, A., and J.M. Graff. 2000. Calmodulin differentially modulates Smad1 and Smad2 signaling. *J. Biol. Chem.* 275:41430–41438. doi:10.1074/jbc.M005727200

Seo, J.H., Y.H. Jin, H.M. Jeong, Y.J. Kim, H.G. Jeong, C.Y. Yeo, and K.Y. Lee. 2009. Calmodulin-dependent kinase II regulates Dlx5 during osteoblast differentiation. *Biochem. Biophys. Res. Commun.* 384:100–104. doi:10.1016/j.bbrc.2009.04.082

Solini, A., S. Cuccato, D. Ferrari, E. Santini, S. Gulinelli, M.G. Callegari, A. Dardano, P. Faviana, S. Madec, F. Di Virgilio, and F. Monzani. 2008. Increased P2X7 receptor expression and function in thyroid papillary cancer: a new potential marker of the disease? *Endocrinology.* 149:389–396. doi:10.1210/en.2007-1223

Stains, J.P., and R. Civitelli. 2005. Gap junctions in skeletal development and function. *Biochim. Biophys. Acta.* 1719:69–81. doi:10.1016/j.bbamem.2005.10.012

Su, M., J.L. Borke, H.J. Donahue, Z. Li, N.M. Warshawsky, C.M. Russell, and J.E. Lewis. 1997. Expression of connexin 43 in rat mandibular bone and periodontal ligament (PDL) cells during experimental tooth movement. *J. Dent. Res.* 76:1357–1366. doi:10.1177/00220345970760070501

Unger, V.M., N.M. Kumar, N.B. Gilula, and M. Yeager. 1999. Three-dimensional structure of a recombinant gap junction membrane channel. *Science.* 283:1176–1180. doi:10.1126/science.283.5405.1176

Vanden Abeele, F., G. Bidaux, D. Gordienko, B. Beck, Y.V. Panchin, A.V. Baranova, D.V. Ivanov, R. Skryma, and N. Prevarskaya. 2006. Functional implications of calcium permeability of the channel formed by pannexin 1. *J. Cell Biol.* 174:535–546. doi:10.1083/jcb.200601115

Vinken, M., T. Vanhaecke, P. Papeleu, S. Snykers, T. Henkens, and V. Rogiers. 2006. Connexins and their channels in cell growth and cell death. *Cell. Signal.* 18:592–600. doi:10.1016/j.cellsig.2005.08.012

Wang, X., H.Y. Kua, Y. Hu, K. Guo, Q. Zeng, Q. Wu, H.H. Ng, G. Karsenty, B. de Crombrugghe, J. Yeh, and B. Li. 2006. p53 functions as a negative regulator of osteoblastogenesis, osteoblast-dependent osteoclastogenesis, and bone remodeling. *J. Cell Biol.* 172:115–125. doi:10.1083/jcb.200507106

Wang, X.H., M. Streeter, Y.P. Liu, and H.B. Zhao. 2009. Identification and characterization of pannexin expression in the mammalian cochlea. *J. Comp. Neurol.* 512:336–346. doi:10.1002/cne.21898

Wicks, S.J., S. Lui, N. Abdel-Wahab, R.M. Mason, and A. Chantry. 2000. Inactivation of smad-transforming growth factor beta signaling by Ca(2+)-calmodulin-dependent protein kinase II. *Mol. Cell. Biol.* 20:8103–8111. doi:10.1128/MCB.20.21.8103-8111.2000

Zayzafoon, M. 2006. Calcium/calmodulin signaling controls osteoblast growth and differentiation. *J. Cell. Biochem.* 97:56–70. doi:10.1002/jcb.20675

Zayzafoon, M., K. Fulzele, and J.M. McDonald. 2005. Calmodulin and calmodulin-dependent kinase IIalpha regulate osteoblast differentiation by controlling c-fos expression. *J. Biol. Chem.* 280:7049–7059. doi:10.1074/jbc.M412680200

Ziganshin, A.U., C.H. Hoyle, G. Lambrecht, E. Mutschler, H.G. Bümert, and G. Burnstock. 1994. Selective antagonism by PPADS at P2X-purinoceptors in rabbit isolated blood vessels. *Br. J. Pharmacol.* 111:923–929.

Downloaded from jcb.rupress.org on May 6, 2012

Supplemental Material can be found at:
http://www.jbc.org/content/suppl/2012/02/01/M111.285874.DC1.html

THE JOURNAL OF BIOLOGICAL CHEMISTRY VOL. 287, NO. 13, pp. 10590–10601, March 23, 2012
Published in the U.S.A.

Role of Epithelial-Stem Cell Interactions during Dental Cell Differentiation*[S]

Received for publication, August 4, 2011, and in revised form, January 5, 2012 Published, JBC Papers in Press, February 1, 2012, DOI 10.1074/jbc.M111.285874

Makiko Arakaki[‡], Masaki Ishikawa[§], Takashi Nakamura[‡], Tsutomu Iwamoto[‡], Aya Yamada[‡], Emiko Fukumoto[‡], Masahiro Saito[¶], Keishi Otsu[‖], Hidemitsu Harada[‖], Yoshihiko Yamada[§], and Satoshi Fukumoto[‡][2]

From the [‡]Division of Pediatric Dentistry, Department of Oral Health and Development Sciences, Tohoku University Graduate School of Dentistry, Sendai 980-8575, Japan, the [§]Laboratory of Cell and Developmental Biology, NIDCR, National Institutes of Health, Bethesda, Maryland 20892, the [¶]Faculty of Industrial Science and Technology, Tokyo University of Science, Chiba 278-8510, Japan, and the [‖]Department of Oral Anatomy II, Iwate Medical College School of Dentistry, Morioka 020-8505, Japan

Background: The role of dental epithelium in stem cell differentiation has not been clearly elucidated.
Results: SP cells differentiated into odontoblasts by epithelial BMP4, whereas iPS cells differentiated into ameloblasts when cultured with dental epithelium.
Conclusion: Stem cells can be induced to odontogenic cell fates when co-cultured with dental epithelium.
Significance: This is the first report to show induction of ameloblasts from iPS cells.

Epithelial-mesenchymal interactions regulate the growth and morphogenesis of ectodermal organs such as teeth. Dental pulp stem cells (DPSCs) are a part of dental mesenchyme, derived from the cranial neural crest, and differentiate into dentin forming odontoblasts. However, the interactions between DPSCs and epithelium have not been clearly elucidated. In this study, we established a mouse dental pulp stem cell line (SP) comprised of enriched side population cells that displayed a multipotent capacity to differentiate into odontogenic, osteogenic, adipogenic, and neurogenic cells. We also analyzed the interactions between SP cells and cells from the rat dental epithelial SF2 line. When cultured with SF2 cells, SP cells differentiated into odontoblasts that expressed dentin sialophosphoprotein. This differentiation was regulated by BMP2 and BMP4, and inhibited by the BMP antagonist Noggin. We also found that mouse iPS cells cultured with mitomycin C-treated SF2-24 cells displayed an epithelial cell-like morphology. Those cells expressed the epithelial cell markers p63 and cytokeratin-14, and the ameloblast markers ameloblastin and enamelin, whereas they did not express the endodermal cell marker Gata6 or mesodermal cell marker brachyury. This is the first report of differentiation of iPS cells into ameloblasts via interactions with dental epithelium. Co-culturing with dental epithelial cells appears to induce stem cell differentiation that favors an odontogenic cell fate, which may be a useful approach for tooth bioengineering strategies.

Tooth morphogenesis is characterized by reciprocal interactions between dental epithelium and mesenchymal cells derived from the cranial neural crest, which result in formation of the proper number and shapes of teeth. Multiple extracellular signaling molecules, including BMPs, FGFs, WNTs, and SHH, have been implicated in these interactions for tooth development (1). Epithelial cells then subsequently give rise to enamel-forming ameloblasts, while mesenchymal stem cells (MSCs)[3] form dentin-forming odontoblasts and dental pulp cells. Initial tooth development is also regulated by extracellular matrices (ECMs), such as basement membrane components that include laminin, collagen, fibronectin, and perlecan (2, 3). These matrices control proliferation, polarity, and attachment, and also determine tooth germ size and morphology. At later stages of tooth development, the basement membrane components disappear and odontogenic cells begin to secrete a variety of tooth-specific extracellular matrices that give rise to layers of enamel and dentin, produced by epithelial-derived ameloblasts and mesenchymal-derived odontoblasts, respectively. Ameloblastin (Ambn) is one of the enamel matrix proteins expressed by differentiating ameloblasts, and is essential for dental epithelial cell differentiation into ameloblasts and enamel formation (2, 4). Dentin sialophosphoprotein (DSPP) is a member of the SIBLING (Small Integrin-Binding Ligand *N*-linked Glycoprotein) family of extracellular matrix glycophosphoproteins, and is expressed by differentiating ameloblasts and odontoblasts (5). These extracellular matrices are important for the formation of enamel and dentin (2).

Stem cell research has identified and established several types of stem cells, including induced pluripotent stem (iPS) cells, which are generated from a variety of somatic cell types via introduction of transcription factors that mediate pluripo-

* This work was supported, in whole or in part, by the Intramural Research Program of the NIDCR, National Institutes of Health (to Y. Y.). This work was also supported by Grants-in-aid 20679006 (to S. F.), 21792054 (to A. Y.), 21792154 (to E. F.) from the Ministry of Education, Science, and Culture of Japan, and the NEXT program (LS010, to S. F.), and by grants from the Takeda Science Foundation.
[S] This article contains supplemental Figs. S1–S5 and Table S1.
[1] Both authors contributed equally to this work.
[2] To whom correspondence should be addressed: Division of Pediatric Dentistry, Department of Oral Health and Development Sciences, Tohoku University Graduate School of Dentistry, Sendai 980-8575, Japan. Fax: 81-22-717-8386; E-mail: fukumoto@dent.tohoku.ac.jp.

[3] The abbreviations used are: MSC, mesenchymal stem cell; mDP, mouse dental pulp; Ambn, Ameloblastin; DSPP, dentin sialophosphoprotein; iPS, induced pluripotent stem; DPSC, dental pulp stem cell; SP, side population; MP, majority population; ALP, alkaline phosphatase; MEF, mouse embryonic fibroblasts; MMC, mitomycin C.

Downloaded from www.jbc.org at TOHOKU UNIVERSITY, on May 6, 2012

tency (6). Direct reprogramming of somatic cells into iPS cells by forced expression of a small number of defined factors (*e.g.* Oct3/4, Sox2, Klf4, and c-Myc) has great potential for tissue-specific regenerative therapies. In addition, this process also avoids ethical issues surrounding the use of embryonic stem (ES) cells, as well as problems with rejection following implantation of non-autologous cells (7). A variety of cell types, including hematopoietic precursor cells (8, 9), endothelial cells, MSCs, neuronal cells (10), reproductive cells (11), and cardiomyocytes (12, 13), undergo *in vitro* differentiation. However previous studies of dental cell differentiation are not adequate to explain this process. Several dental stem cell populations have been identified in different parts of the tooth, including cells from the periodontal ligament that links the tooth root with the bone, tips of developing roots, and tissue (dental follicle) that surrounds an unerupted tooth. In addition, dental pulp stem cells (DPSCs) have been identified in the pulp of exfoliated deciduous teeth of both children and adults (14). These different cell types likely share a common lineage, being derived from neural crest cells, and all have generic MSC-like properties.

Transplantation of *in vitro* expanded DPSCs mixed with hydroxyapatite/tricalcium phosphate particles results in the formation of dental pulp and dentin-like tissue complexes in immunocompromised mice (15). Similar results have been observed with an MSC population obtained from human exfoliated deciduous teeth (SHED) (14). DPSCs also express the putative stem cell marker STRO-1 and perivascular cell marker CD146, while a proportion co-expresses smooth muscle actin and the pericyte-associated antigen 3G5 (16). These findings suggest that a population of DPSCs may reside in this perivascular niche within the pulp of adult teeth.

Side population (SP) cells were identified by flow cytometry analysis with a Hoechst 33342 efflux assay and found to have stem cell characteristics (17). SP cells are a small population that show low levels of Hoechst dye staining for the expression of Abcg2, an ATP-binding cassette transporter (18), which is strongly expressed in dental pulp in human adult and deciduous teeth (19). Dental pulp contains multipotent stem cells and is viewed as a potential source of iPS cells (14, 20, 21). In tooth germ development, undifferentiated neural crest-derived MSCs interact with dental epithelium and differentiate into dentin matrix-secreting odontoblasts. However, the interactions between stem cells and dental epithelium have not been clearly elucidated.

In this study, we established an SP cell line from mouse dental papilla. We then cultured these SP cells with rat dental epithelial cells to investigate epithelial-mesenchymal interactions. SP cells were induced to differentiate into DSPP expressing odontoblasts via the action of epithelial BMP4. Furthermore, mouse iPS cells differentiated into Ambn-expressing dental epithelium when cultured with dental epithelial cells. Thus, these undifferentiated stem cells can be induced to an odontogenic cell fate when co-cultured with dental epithelial cells. These findings may be useful for analysis of dental cell differentiation *in vitro* and for procurement of odontogenic cells for use in regenerative medicine.

EXPERIMENTAL PROCEDURES

Preparation of Mouse Dental Papilla Cells—Dental papilla tissues were isolated from incisors from newborn ICR mice by digesting with 0.1% collagenase D (Roche) and 2.5% trypsin for 30 min at 37 °C. Enzymatically digested tissues were minced into 2–4 mm pieces using micro-scissors and washed three times with Dulbecco's modified Eagle's medium (DMEM) (Invitrogen) containing 10% fetal bovine serum (FBS) (Invitrogen) and an antibiotic-antimycotic mixture (Invitrogen), then filtered through a cell strainer (40 μm) to eliminate clumps and debris. Mouse dental papilla (mDP) cells were cultured in 60-mm culture dishes and immortalized by expression of a mutant human papilloma virus type 16 E6 gene lacking the PDZ-domain-binding motif (22). mDP cells were maintained with DMEM supplemented with 10% FBS and an antibiotic-antimycotic mixture at 37 °C in a humidified atmosphere containing 5% CO_2.

Generation of Dental Epithelial Cell Line SF2-24 and Cell Culture—Rat dental epithelial cells were enzymatically isolated from the cervical loop at the apical end of the lower incisors from a Sprague-Dawley rat with 1% collagenase. Dental epithelial cells were cultured with DMEM (Invitrogen) supplemented with 10% FBS for 4 weeks, then, maintained in serum-free keratinocyte synthetic medium (Keratinocyte-SFM, Invitrogen) for 1 year. An established cell line, SF2 was maintained as previously described (4). SF2 cells were transfected with a pEF6/GFP-PDGFtm-myc-HA vector expressing the GFP-PDGF receptor-transmembrane fusion protein with myc-HA tag using Lipofectamine 2000 (Invitrogen). Transfected cells were selected as SF2 subclones by culturing with media containing 400 μg/ml of G418. Twenty-five clones were selected as a stable transfected cell line, with one of them designated as SF2-24 (Ambn high expression) and another SF2-7 (Ambn low expression).

SP and MP Cell Analysis and Flow Cytometry—Hoechst staining of mDP cells for SP cell analysis was conducted as previously described (17). Subconfluent mDP cells were stained with Hoechst dye for 90 min at 37 °C. After staining, all cells were resuspended in 100 μl of Hanks' balanced salt solution (HBSS) with calcium/magnesium medium and kept on ice. The SP and MP gates were defined as previously described (17). For analysis, the cells were resuspended in ice-cold HBSS with 2% FBS containing propidium iodide (Sigma) at a final concentration of 2 μg/ml to identify dead cells, then filtered through a cell strainer. Sorting and analyses were carried out with an EPICS ALTRA flow cytometer (Beckman Coulter, Fullerton, CA). The SP cell fraction was enriched by repeating cell sorting 3 times. The expression of stem cell markers in SP cells was confirmed by flow cytometry using anti-Sca-1 and Oct3/4 antibodies (Santa Cruz Biotechnology).

Differentiation of SP Cells—For odontoblastic induction, SP cells were plated at 6×10^4 cells in 60-mm dishes. After the cells had reached 50–60% confluence, we replaced the control medium with induction medium containing 100 ng/ml of BMP2 or BMP4 (Wako Pure Chemical Industries), and cells were incubated for 2 days. For blocking BMP signaling, recombinant mouse Noggin protein (R&D systems) was

Downloaded from www.jbc.org at TOHOKU UNIVERSITY, on May 6, 2012

used. Total RNA was isolated and real time RT-PCR was performed using mouse Bcrp1 (18) and DSPP primer sets (supplemental Table S1).

For adipogenic differentiation, SP cells were seeded at 1×10^5 cells per well in 6-well plates and cultured in DMEM supplemented with 10% FBS. Adipogenic differentiation was induced with induction medium from a Poietics hMSC Media Bullet kit (Cambrex Bio Science Walkersville, Inc., Walkersville, MD) for 3 days and incubated in maintenance medium for 3 days, then the cells were cultured for an additional 7 days in maintenance medium. As a control, cells were cultured in only maintenance medium. Adipogenesis was confirmed by staining with Oil-Red-O and the expression of *PPARγ* was analyzed by RT-PCR.

For osteogenic differentiation, SP cells were seeded at 1.5×10^4 cells per well in 6-well plates and cultured in DMEM supplemented with 10% FBS, 10 mM β-glycerophosphate, 0.2 mM ascorbic acid, 2-phosphate, and 10^{-8} M dexamethasone. Induction and control media were replaced every 2 days. Osteogenesis was determined by alkaline phosphatase (ALP) and von Kossa staining for calcium deposition, as previously described (23). After 4 weeks culturing with osteoblast induction medium, the expressions of osteocalcin, osteonectin, and Runx2 in osteogenesis-induced SP cells were analyzed by RT-PCR.

For neurogenic differentiation, we modified a neuronal induction protocol using recombinant nerve growth factor (NGF) (Chemicon). SP cells were seeded at 1×10^5 cells per well in 6-well plates. After reaching 80–90% confluence, neurogenic differentiation was induced by culturing the cells in DMEM supplemented 2% FBS, 1.25% dimethyl sulfoxide, 10^{-6} M retinoic acid, 2.5 μg/ml insulin, and 50 ng/ml NGF. Two weeks later, neurogenesis was characterized by Western blot analysis using an anti-neurofilament-M specific antibody (Cell Signaling Technology).

Odontoblastic Induction of SP Cells by Co-culturing with Dental Epithelial Cells—We investigated the role of dental epithelial cells in specification of odontogenic cell lineage using two types of co-culture systems: feeder and chamber types with a cell culture insert (BD Falcon). We used confluent SF2 cells, or SF2 cells treated with 4% paraformaldehyde (PFA) or ammonium (denudation) as feeder cells. SF2 and SP cells were harvested and placed into either 6-well plates or cell culture inserts (chamber), then cultured until reaching confluence.

Screening of Co-culture Conditions for Ameloblastic Induction of iPS Cells—A mouse iPS cell line (iPS-MEF-Ng-20D-17), carrying the Nanog-GFP/IRES/puromycin resistant gene, was established by Yamanaka (Kyoto University, Japan), and obtained from RIKEN Cell Bank (Saitama, Japan) (6). Mouse iPS cells were cultured with rat dental epithelial cells (SF2-24), which predominantly express Ambn mRNA, as feeder cells. Preparatory co-culture experiments were performed as follows: iPS cells were cultured with mouse embryonic fibroblasts (MEFs) treated with mitomycin C (MMC) or with three different types of SF2-24 feeder cells (confluent cells, cells treated with MMC, cells treated with 4% PFA). MMC was supplied at 9 μg/ml (final concentration) for 2 h to arrest SF2-24 cell proliferation.

Induction of iPS Cell-derived Ameloblasts—iPS cells (plated $1.5 \times 10^3/cm^2$) were cultured on sheets of MMC-treated SF2-24 cells for 7, 10, and 14 days in the same medium used for the SF2-24 culture without leukemia inhibitory factor and 2-mercaptoethanol. The culture medium was changed every day throughout the co-culture period. After 7 and 10 days, the co-cultured iPS cells were subjected to RT-PCR, while those after 14 days of culture were analyzed by immunocytochemistry. Total RNA from iPS cells co-cultured with MMC-treated MEFs was isolated after 3 days of culture. Conditioned media from cultures of SF2-24 and SF2-7 were collected after 2 days of incubation. The procedures used for transfection of Ambn-expressing vectors, as well as their construction and isolation of recombinant proteins have been previously described (2, 24). K252a (Trk inhibitor, Calbiochem), PD98059 (MEK inhibitor, Cell signaling), anti-NT-4 neutralizing antibody (Applied Biological Materials), and Noggin (R&D systems) were added to conditioned medium obtained from SF2-24 cells.

Reverse Transcription-PCR—Total RNA was isolated using TRIzol (Invitrogen) and first-strand cDNA was synthesized at 50 °C for 50 min using oligo(dT) or random primers with the SuperScript III First-strand Synthesis System (Invitrogen). PCR was performed with Takara Ex Taq HotStart Version (Takara) or a PCR Additives Kit (Jena Bioscience, Germany). The primer sequences are presented in supplemental Table S1. PCR amplicons were separated and visualized on 1.5% agarose gels with SYBR Green staining using the LAS-4000 mini image analyzing system (Fujifilm). For semi-quantitative PCR analysis, the band intensities of PCR amplicons were quantified using MultiGauge software (Fujifilm) and normalized by dividing the intensity of the band of GAPDH. Because of the high degree of homology between the Ambn gene in mice and rats (94.2%), we designed a species-specific mouse Ambn primer that encoded locked nucleic acid (LNA) at a different base sequence between the mouse and rat Ambn gene in a conserved region. The specificity of the mouse Ambn primer was confirmed by PCR using mouse and rat tooth germ cDNA. Statistical analysis of gene expression was performed using the Student's *t* test.

Immunocytochemistry—For immunocytochemistry, cells were fixed with 4% PFA for 5 min at room temperature. After washing with PBS three times for 5 min, the cells were treated with Power Block Universal Reagent (BioGenex) for 5 min at room temperature, followed by three washes with PBS. The cells were incubated with the anti-Ambn primary antibody included in the kit (1:200, M-300, Santa Cruz Biotechnology). The primary antibody was visualized with Alexa Fluor 594 donkey anti-rabbit antibody (1:500, A21207, Invitrogen). Nuclei were stained with Hoechst 33258 (Invitrogen). Immunocytochemistry and phase images were captured using a BZ-8000 microscopic system (KEYENCE Co, Osaka, Japan), and images of the sections were analyzed using a BZ analyzer (KEYENCE).

RESULTS

Establishment of SP Cell Line from Mouse Dental Papilla Cells—Side population (SP) cells, which displayed stem cell ability, make up less than 1% of total cells in the mouse dental papilla (mDP) from postnatal tooth germs. Thus, biochemical and biomolecular analyses of SP cells are difficult to perform

Downloaded from www.jbc.org at TOHOKU UNIVERSITY, on May 6, 2012